

A coupling-based approach to f -divergences diagnostics for Markov chain Monte Carlo

Adrien Corenflos¹ and Hai-Dang Dau²

¹Department of Statistics, University of Warwick

²Department of Statistics and Data Science, National University of Singapore
adrien.corenflos@warwick.ac.uk, hddau@nus.edu.sg

October 16, 2025

Abstract

A long-standing gap exists between the theoretical analysis of Markov chain Monte Carlo convergence, which is often based on statistical divergences, and the diagnostics used in practice. We introduce the first general convergence diagnostics for Markov chain Monte Carlo based on any f -divergence, allowing users to directly monitor, among others, the Kullback–Leibler and the χ^2 divergences as well as the Hellinger and the total variation distances. Our first key contribution is a coupling-based ‘weight harmonization’ scheme that produces a direct, computable, and consistent weighting of interacting Markov chains with respect to their target distribution. The second key contribution is to show how such consistent weightings of empirical measures can be used to provide upper bounds to f -divergences in general. We prove that these bounds are guaranteed to tighten over time and converge to zero as the chains approach stationarity, providing a concrete diagnostic. Numerical experiments demonstrate that our method is a practical and competitive diagnostic tool.

Keywords— Markov chain Monte Carlo; Couplings; Diagnostics; Effective sample size; Chi-squared divergence; Importance weights

1 Introduction

1.1 Markov chain Monte Carlo and convergence diagnostics

Computing the expectation $\pi(\varphi) = E_\pi(\varphi)$ of a test function φ with respect to a distribution π of interest is routinely achieved by means of Markov chain Monte Carlo (MCMC, see, e.g., Brooks et al., 2011). This class of methods generates samples $X_{t+1} \sim K(X_t, \cdot)$ under a Markov kernel K designed to keep π invariant: $(\pi K)(dy) = \int K(x, dy)\pi(dx) = \pi(dy)$. Expectations under π are then often computed in one of two compatible ways: either by averaging over the iterations generated by the Markov chain, $\pi(\varphi) \approx \sum_{t=B}^T \varphi(X_t)/(T - B + 1)$; or by combining $N > 1$ such independent estimates $\hat{\varphi}^n = \sum_{t=B}^T \varphi(X_t^n)/(T - B + 1)$ together as $\pi(\varphi) \approx \sum_{n=1}^N \hat{\varphi}^n/N$. Here $B > 0$ is a ‘burn-in’ period, used to discard the initial samples of the Markov chain, which are often not representative of the target distribution π . Under technical conditions on the initial distribution of $X_0 \sim \mu_0$, the kernel, and the target, the marginal distribution μ_t of X_t converges to π as $t \rightarrow \infty$. Such results are typically obtained in terms of the rate of decay of the total variation distance $\|\mu_t - \pi\|_{\text{TV}}$ between the two distributions, or of the Wasserstein distance (see, e.g., Meyn and Tweedie, 2009; Douc et al., 2018). However, despite their elegant theoretical foundations, these results are hardly amenable to practical use, as they often make use of non-accessible properties of the target distribution π .

Diagnostic tools for MCMC have therefore historically drifted away from the theoretical metrics highlighted above, focusing instead on more accessible and interpretable quantities that can provide guidance for practitioners. Central among these is the Gelman–Rubin diagnostic (Gelman and Rubin, 1992), which, from N independent simulations $X_{0:T}^{1:N}$, tests whether all chains agree about their estimate $\sum_{t=0}^T \varphi(X_t^n)/(T + 1)$ of $\pi(\varphi)$. This method, refined over the years (Vats and Knudson, 2021; Vehtari et al., 2021) has been very successful, in part due to its

integration to software packages, its ease of use in practice, and the fact that it provides an estimator of the *effective sample size* of a test statistic:

$$\text{ESS} = \frac{T + 1}{1 + 2 \sum_{t=0}^T \text{corr}\{\varphi(X_0), \varphi(X_t)\}}.$$

This effective sample size is interpreted as the number of independent samples from π that would yield the same variance as exhibited by the Markov chain $X_{0:T}$ for φ . Nonetheless, it is not without limitations: it directly targets a specific aspect of the convergence of the Markov chain, namely the agreement in terms of a specific functional, rather than a more fundamental property of the chain itself. While this may serve as a surrogate (for example when φ is a collection of moments), it does not provide a complete picture of the convergence behaviour of the chain.

Complementary to Gelman–Rubin-style diagnostics, few but important monitoring tools have been proposed that directly assess the convergence of the Markov chain to stationarity in terms of a given metric, always either the total variation or the Wasserstein distance, as far as we are aware. A notable example is Biswas et al. (2019) who obtain generally applicable and computable (via Monte Carlo) upper bounds to both distances. Their method is based on a debiasing technique using coupled Markov chains, originating from Glynn and Rhee (2014); Jacob et al. (2020b). For instance, for the total variation, $\|\mu_t - \pi\|_{\text{TV}}$ can be upper bounded by $E\{(\lceil \tau \rceil - L - t)/L\}$, where $\tau = \min(t > L \mid X_t = Y_{t-L})$ and $(X_t)_{t \geq 0}$ and $(Y_t)_{t \geq 0}$ are marginally distributed according to the same Markov chain. Implementing such a method in practice often amounts to designing a coupling between the two lagged chains, $\bar{K}(x_t, y_{t-L}, dx_{t+1}, dy_{t+1-L})$ under which τ is almost surely finite. Many such couplings have since been proposed in the literature, covering a range of popular kernels (see Ceriani and Zanella 2024; Heng and Jacob 2019; Jacob et al. 2020a; Lee et al. 2020; Corenflos et al. 2025; Papp and Sherlock 2024; Wang et al. 2021; Biswas et al. 2022 and Section I for a longer discussion). Still, the total variation and the Wasserstein distances are difficult to interpret on their own, which limits their applicability in practical scenario: given the information that $\|\mu_t - \pi\|_{\text{TV}} < \epsilon$, practitioners may find it challenging to determine the implications for their specific problem. Additionally, the lag $L > 0$ is a hyperparameter chosen such that X_L is approximately at stationarity. Choosing it ahead of time is therefore a somewhat circular exercise as it can be picked based on an upper bound that depends upon it. In other terms, Biswas et al. (2019) is likely more useful as an alert tool, providing warnings when the Markov chain does not converge, or as a comparison tool, where different kernels can be pitched together, rather than as an actionable quantity in the case when it does converge.

On the other hand, if we knew the Radon–Nikodym derivative $d\pi/d\mu_t$ (which in most cases of interest is equivalent to the ratio of their densities), we could obtain consistent estimates of π from a μ_t -distributed sample using the celebrated *importance sampling* procedure (dating at least from Kahn and Harris, 1951). In addition, we could estimate any statistical divergences of π with respect to μ_t provided that they are defined solely in terms of the Radon–Nikodym derivative. This class of divergences, called f -divergences (Rényi, 1961), includes popular objectives such as the Kullback–Leibler divergence (KL), the total variation distance (TV), and the Rényi divergences. Unfortunately the exact ratio $d\pi/d\mu_t$ is intractable in all but the most trivial cases.

1.2 Contributions

In this article we propose a novel way to run parallel MCMC chains which gives a consistently weighted approximation of π at each time step. These can be interpreted as noisy approximations of the Radon–Nikodym derivative $d\pi/d\mu_t$. We leverage this construction to introduce upper bounds to the f -divergences of the target with respect to the current sample distribution. Contrary to existing diagnostics, our method is fully online and valid from step one, requiring no lag or warm-up. A key consequence stemming from the connection between the χ^2 -divergence and the effective sample size, is that we can estimate the ‘effective number of active chains’, a highly interpretable and practical diagnostic for practitioners. Our construction is based on Markov kernel coupling techniques arising from the MCMC (Glynn and Rhee, 2014; Jacob et al., 2020b) literature and a weighting structure arising from sequential Monte Carlo literature (see e.g. Chopin and Papaspiliopoulos, 2020), in particular Dau and Chopin (2023, Section 4.2) using two interacting copies of N independent chains.

The rest of the article is organized as follows. Section 2 explains how any weighted approximation of the target can be used as a diagnostic and highlights the challenge of finding a good one in the context of MCMC. Section 3 details our method, termed weight harmonization, and explains how it can be used both to diagnose the convergence of MCMC and to produce a consistent estimate of expectations under the target for any finite t . Section 4 provides consistency and unbiasedness results for the resulting importance weighted MCMC chains. Additionally, under strong mixing assumptions and a coupling assumption akin to uniform ergodicity, we prove that the system of weights converges exponentially fast to uniform weighting of all trajectories, recovering a computational version of exponential ergodicity theorems and validating the use of our method as a diagnostic. Section 5 illustrates the empirical behaviour of our method and shows that it returns practical albeit conservative estimators of the effective sample size of the system. Section 6 concludes with a discussion of different advantages and drawbacks

of our method. In particular, we identify two likely points of improvement: increasing the interaction between particles by Rao–Blackwellization, and offline correction of the estimators, in a fashion similar to particle smoothing operations (see, e.g., Dau and Chopin, 2023; Chopin and Papaspiliopoulos, 2020, Chapter 12).

1.3 Notations and conventions

Let $\pi(x) = \gamma(x)/Z$ be a target distribution known up to its normalizing constant $Z = \int \gamma(x)dx$. We consider given a π -invariant (and therefore γ -invariant) Markov kernel $K(x, \cdot)$: $\pi K = \pi$. Couplings over K are defined as joint constructions $X', Y' \sim \bar{K}(x, y, \cdot, \cdot)$, which marginally verify $(X' \mid x) \sim K(x, \cdot)$ and $(Y' \mid y) \sim K(y, \cdot)$. We write $K^t(x, \cdot) = \int \int \cdots \int K(x_t, \cdot)K(x_{t-1}, dx_t) \cdots K(x, dx_1)$ for K applied t times, with $K^1 = K$ and $K^0 = \delta_x(dx)$ being the identity kernel. When μ is a probability measure and K is a Markov kernel, we write $\mu \times K$ for the joint $\mu(dx)K(x, dy)$.

We use subscript for time index and superscript for sample index: X_t^n is the particle n evolved until time t . Collections over both indices are written as $X_{0:t}^{1:N}$, the set of all N ‘trajectories’ $(X_{0:t}^n)_{n=1}^N$ over the time interval $(0 : t) = 0, \dots, t$.

Markov chains are started using samples from a tractable distribution $\mu = \mu_0$, and we write $\mu_t = \mu K^t$ for the marginal distribution of the chain at time t . Similarly, we write $K\varphi: x \mapsto \int \varphi(y)K(x, dy)$ for the action of K on a measurable test function φ .

Gaussian distributions are denoted as $\mathcal{N}(\mu, \Sigma)$, where μ and Σ are the mean and covariance of the distribution, respectively. We do not distinguish between the multivariate and the univariate cases. The vector of n ones is denoted 1_n , the vector of n zeroes 0_n , and we write I_n for the identity matrix of size n .

2 Importance weighting and Markov chain

2.1 f-divergences and effective sample size

We first recall the definition of f -divergences, apply it to discrete representations, and define the notation of effective sample size.

Definition 1. Let μ and π be two probability distributions and let $f: [0, \infty) \rightarrow [-\infty, \infty]$ be a convex function such that $f(1) = 0$. The f -divergence of π with respect to μ is defined by

$$D_f(\pi \parallel \mu) = \int \mu(dx) f\left\{ \frac{d\pi}{d\mu}(x) \right\}.$$

Example 1. Typical examples of f -divergences include the Rényi divergences for $f(t) = |t - 1|^\alpha$, total variance distance for $f(t) = |t - 1|/2$, the Kullback-Leibler divergence for $f(t) = t \log t$, the reverse Kullback-Leibler for $f(t) = -\log t$, and the squared Hellinger distance for $f(t) = (\sqrt{t} - 1)^2/2$. (In these examples, the value of f at 0 is implicitly defined as $\lim_{t \rightarrow 0^+} f(t)$ if needed, and could be equal to plus or minus infinity.) We will pay particular attention to the chi-squared distance, denoted by χ^2 , which is the Rényi divergence for $\alpha = 2$ and corresponds to $f(t) = (t - 1)^2$.

The following immediate lemma applies Definition 1 to the case of discrete measures.

Lemma 1. Let W^1, \dots, W^N be N non-negative real numbers such that $\sum_{n=1}^N W^n = 1$. Then, for any N elements X^1, \dots, X^N in an arbitrary space \mathcal{X} ,

$$D_f\left(\sum_{n=1}^N W^n \delta_{X^n}, \frac{1}{N} \sum_{n=1}^N \delta_{X^n}\right) = \frac{1}{N} \sum_{n=1}^N f(NW^n). \quad (1)$$

In particular, for the chi-squared distance where $f(t) = (t - 1)^2$,

$$\chi^2\left(\sum_{n=1}^N W^n \delta_{X^n}, \frac{1}{N} \sum_{n=1}^N \delta_{X^n}\right) = N \sum_{n=1}^N (W^n)^2 - 1. \quad (2)$$

This corollary is particularly appealing in the scenario where X^1, \dots, X^N are independent draws from μ and the weights W^n are proportional to $d\pi/d\mu(X^n)$. Then under mild conditions (1) converges to $D_f(\pi \parallel \mu)$ and in particular (2) converges to $\chi^2(\pi \parallel \mu)$.

An alternative way of characterizing the chi-squared distance on discrete measures is the effective sample size (Kong et al., 1994), defined on the weights $W^{1:N}$ as

$$\text{ess}(W^{1:N}) = \frac{1}{\sum_{n=1}^N (W^n)^2}, \quad (3)$$

which relates to the ‘theoretical’ effective sample size

$$\text{ess}^*(N) = \frac{N}{\chi^2(\pi||\mu) + 1}. \quad (4)$$

The more ‘uniform’ the weights are, the higher the effective sample size is, and the lower the discrete chi-squared divergence in (2) becomes. In particular, a zero chi-squared divergence corresponds to an effective sample size of N , the maximum possible value, obtained when all the weights are equal to $1/N$. The effective sample size can be interpreted as quantifying the number of active particles (Chopin and Papaspiliopoulos, 2020, Section 8.6): if k weights are zero, and the rest are all equal to one another, then the resulting effective sample size will be $N - k$.

Assumption 1. The function f is continuous on $(0, \infty)$. Moreover, it is continuously differentiable everywhere on $(0, \infty)$ except for at most one point c , at which we define $f'(c) := \{\lim_{t \rightarrow c^-} f'(t) + \lim_{t \rightarrow c^+} f'(t)\}/2$.

We assume that this condition holds throughout the paper. All the divergences in Example 1 satisfy this assumption.

2.2 Weighted approximations as diagnostics

A central object in our methodology is the class of weighted approximations of the target distribution. Let X^1, \dots, X^N be N (not necessarily independent) identically distributed draws from a distribution μ . We are most interested in the case where $\mu = \mu_t = \mu_0 K^t$ is the distribution of a Markov chain state after t iterations of a π -invariant MCMC kernel K when started at μ_0 . Suppose further that we have N random weights W^1, \dots, W^N such that $\sum_{n=1}^N W^n = 1$ and

$$\sum_{i=1}^N W^n \varphi(X^n) \rightarrow \int \varphi(x) \pi(dx) \quad (5)$$

converges in probability, for all functions φ in a reasonably large function class Φ . We say that $\sum_{n=1}^N W^n \delta_{X^n}$ is a *weighted representation* of π . The following theorem shows how this consistent approximation can be turned into a convergence diagnostic.

Write $\psi = d\pi/d\mu$ for the Radon–Nikodym derivative of π with respect to μ .

Assumption 2. The weights W^n are such that $\sum_{n=1}^N W^n f'(\psi(X^n)) \rightarrow \int f'(\psi(x)) \pi(dx)$ in probability as $N \rightarrow \infty$.

Assumption 3. The unweighted empirical measure satisfies the weak law of large numbers for $x \mapsto f(\psi(x))$ and $x \mapsto \psi(x) f'(\psi(x))$:

$$\frac{1}{N} \sum_{n=1}^N f(\psi(X^n)) \rightarrow \int f(\psi(x)) \mu(dx), \quad \frac{1}{N} \sum_{n=1}^N \psi(X^n) f'(\psi(X^n)) \rightarrow \int \psi(x) f'(\psi(x)) \mu(dx),$$

where both convergences are in probability for $N \rightarrow \infty$.

Theorem 1. Under Assumptions 1, 2, and 3, for any fixed $\varepsilon > 0$ we have, as $N \rightarrow \infty$,

$$\text{pr} \left\{ \frac{1}{N} \sum_{n=1}^N f(NW^n) \leq D_f(\pi||\mu) - \varepsilon \right\} \rightarrow 0.$$

In plain English, Theorem 1 states that the probability that a consistent weighted approximation of (1) gives an *underestimate* of an f -divergence is vanishingly small, and thus it can serve as an *upper bound* with high probability. When the particles $X^{1:N}$ are independent, the ideal weights are

$$W^n = \frac{(d\pi/d\mu)(X^n)}{\sum_{i=1}^N (d\pi/d\mu)(X^i)},$$

for which it can be straightforwardly checked that the degree of overestimation is asymptotically zero, i.e., that, under regularity conditions, $\sum_{n=1}^N f(NW^n)/N$ converges to $D_f(\pi||\mu)$ almost surely.

2.3 Naive approximation in MCMC and its suboptimality

Consider N independent parallel MCMC chains $(X_{0:T}^n)$ for $n = 1, \dots, N$ where $X_0 \sim \mu_0$ and $X_{t+1}^n \sim K(x, \cdot_t^n)$. Write

$$W_0^n = \frac{(\mathrm{d}\pi/\mathrm{d}\mu_0)(X_0^n)}{\sum_{i=1}^N (\mathrm{d}\pi/\mathrm{d}\mu_0)(X_0^i)},$$

which is tractable because the quantity does not depend on the normalizing constant of π . Then it is straightforward to show that, under mild conditions,

$$\sum_{n=1}^N W_0^n \varphi(X_t^n) \rightarrow \int \varphi(x) \pi(\mathrm{d}x)$$

for any $t \geq 0$. In particular, Theorem 1 says that the f -divergence of π with respect to μ_t , for *any* t , can be asymptotically upper-bounded by $\sum_{n=1}^N f(NW_0^n)/N$. This bound is clearly suboptimal since it does not vary in t and does not take into account the mixing of the Markov chain. We now present a scheme where the weights are ‘harmonized’ as the Markov chain progresses, reflecting its mixing through the notion of coupling.

3 Weight-harmonization via couplings

3.1 Couplings of Markov kernels

In Section 2.3, we considered MCMC chains running independently in parallel. In particular, for target distributions with Lebesgue density in \mathbb{R}^d and popular MCMC algorithms, such as most forms of Metropolis–Hastings-corrected dynamics (Metropolis et al., 1953), the states of two distinct chains will almost surely not coincide. Formally, for continuous state-spaces the *independent coupling* $\tilde{K}_{\text{ind}}(x, y, \mathrm{d}x', \mathrm{d}y') = K(x, \mathrm{d}x')K(y, \mathrm{d}y')$ is such that $\text{pr}(X' = Y' \mid X, Y) = 0$ for any $X \neq Y$. It is however possible to design couplings $\tilde{K}(x, y, \mathrm{d}x', \mathrm{d}y')$ such that the meeting probability can be positive, while each chain taken in isolation still behaves as an ordinary Markov chain, i.e. the marginal $\tilde{K}(x, y, \mathrm{d}x') = K(\mathrm{d}x, \mathrm{d}x')$ does not depend on y and $\tilde{K}(x, y, \mathrm{d}y') = K(y, \mathrm{d}y')$ does not depend on x . In Appendix I, we detail some such couplings for usual MCMC algorithms.

The key idea of our method is the following: given a set of N chains, we can make them interact pairwise via coupled kernels. When two Markov chains, associated with different weights, eventually collapse to the same state (we say they meet or couple), they can then split even their previous weights and be reallocated to other peer chains. As the simulation progresses, more meeting events will take place between different chains and therefore equalize the weights of all chains present.

3.2 Equalizing weights of coupled particles

Our scheme relies on the notion of ‘couples’, as such it is more convenient to work with a system of $2N$ instead of N draws. Consider a π -invariant kernel $K(x, \mathrm{d}x')$ and a coupling \tilde{K} of K with itself. In this setting, let $\sum_{n=1}^{2N} W_t^n \delta_{X_t^n}$ be a weighted representation, in the sense of (5), of π for a population $X_t^{1:2N}$ distributed identically according to μ_t . We can construct a new particle representation of π as $\sum_{n=1}^{2N} W_t^n \delta_{X_{t+1}^n}$, where X_{t+1}^n, X_{t+1}^{n+N} is obtained by applying independently the kernel \tilde{K} to the pairs (X_t^n, X_t^{n+N}) , for $n = 1, \dots, N$. It is easy to see that, regardless of the choice of coupling, the resulting particle representation is still a valid representation of the target distribution π .

Now, assume that, under the coupled simulation, we obtain $X_{t+1}^n = X_{t+1}^{n+N}$ for some $n \in \{1, \dots, N\}$, then

$$W_t^n \delta_{X_{t+1}^n} + W_t^{n+N} \delta_{X_{t+1}^{n+N}} = \{\alpha W_t^n + (1 - \alpha) W_t^{n+N}\} \delta_{X_{t+1}^n} + \{(1 - \alpha) W_t^n + \alpha W_t^{n+N}\} \delta_{X_{t+1}^{n+N}} \quad (6)$$

for any $\alpha \in [0, 1]$. In the rest of this paper, we will take $\alpha = 1/2$. This formulation allows us to combine the weights of the two particles into a unique shared weight, reducing the variability of the weights and thus hopefully decreasing the f -divergence upper bound as per Theorem 1. In Appendix C, we derive an upper bound on the maximum improvement of effective sample size (3) we can ever achieve after one step of weight harmonization, and the motivation behind the choice $\alpha = 1/2$.

Remark 1. Under the weight update rule (6), $\sum_{n=1}^{2N} W_{t+1}^n = \sum_{n=1}^{2N} W_t^n = 1$. In fact, while we have written the procedure over normalized weights, exactly the same operation can be performed over un-normalized weights:

$$w_{t+1}^n = w_t^n, \quad n \in \{1, \dots, 2N\} \setminus \{j, j+N\}, \quad \text{and} \quad w_{t+1}^j = w_{t+1}^{j+N} = (w_t^j + w_t^{j+N})/2.$$

In this case, normalizing after the fact: $\tilde{W}_{t+1}^n = w_{t+1}^n / \sum_{m=1}^{2N} w_{t+1}^m$ will yield exactly the same result as applying the update on the normalized weights directly: $\tilde{W}_{t+1}^{1:2N} = W_{t+1}^{1:N}$. This is because the sum of the weights $\sum_{m=1}^{2N} w_{t+1}^m = \sum_{m=1}^{2N} w_t^m$ is unchanged by the harmonization operation.

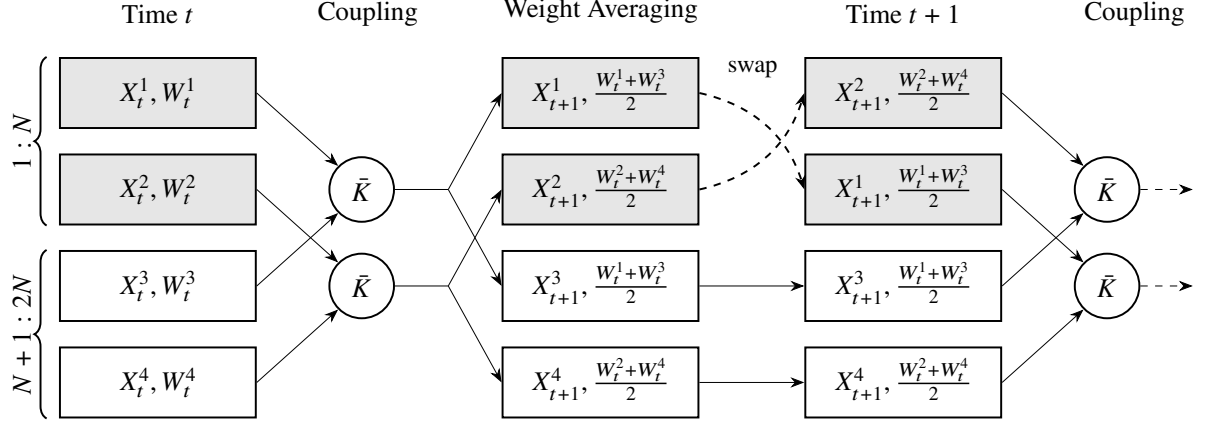


Figure 1: Step of Algorithm 1 for $2N = 4$ particles and successful couplings: $X_{t+1}^1 = X_{t+1}^3$ and $X_{t+1}^2 = X_{t+1}^4$.

3.3 Exchanging pairs of particles

Of course, coupling the same particles over and over again will result in N pairs of equal particles, but will not modify the weights of the particles across these pairs. In our notations, repeatedly coupling X_t^n and X_t^{n+N} for all t might eventually result in $W_t^n = W_t^{n+N}$ for t large enough, but not $W_t^n = W_t^m$ for $1 \leq m < n \leq N$ since the m -th and n -th chains would have no chance to communicate. We therefore need to introduce the exchange of information, which we do by randomizing the pairings of particles. More precisely, given the particles $X_{t+1}^{1:N}$, we do not couple the one at index n with the one at index $n+N$, but the one with index n with the one at index $A_{t+1}^n + N$ for a time-changing permutation $A_s^{1:N}$ of $\{1, \dots, N\}$, $s \geq 0$. We determine $A_{t+1}^{1:N}$ from the previous pairing $A_t^{1:N}$ with two objectives in mind: pairs that have not yet coupled should be left alone, and pairs that have coupled should be exchanged whenever possible. This amounts to setting $A_{t+1}^{1:N}$ to a modification of the array $A_t^{1:N}$ where the subset of coupled indices is permuted and the rest of the indices are left intact. The algorithmic description of the method is given in Algorithm 1 while a more intuitive visual illustration is given in Figure 1.

Remark 2. We have written Algorithm 1 in terms of normalized weights $W^{1:2N}$, but as per Remark 1, this can be written directly in terms of the un-normalized weights with no impact on the downstream representation.

The initialization of the method is given by simply taking independent samples from an initial distribution μ_0 and weighting them accordingly as $X_0^n \sim \mu_0(dx)$, $w_0^n = \gamma(X_0^n)/\mu_0(X_0^n)$, and $W_0^n = w_0^n / \sum_{m=1}^{2N} w_0^m$ for $n = 1, \dots, 2N$,

3.4 Interpretation and usage

At each step, the algorithm produces $2N$ draws $X_t^{1:2N}$ and weights $W_t^{1:2N}$. We will prove in Section 4 (Theorem 2) that the normalized weights satisfy

$$\sum_{n=1}^{2N} W_t^n \varphi(X_t^n) \rightarrow \int \varphi(x) \pi(dx)$$

for a reasonably large class of function φ , where the convergence is in probability as $N \rightarrow \infty$. As such the particles and their weights can be used to consistently approximate expectations under the target distribution. Additionally, we will also prove (Corollary 2) that, under ergodicity conditions, the weights themselves converge to the equal weights $W_t^{1:2N} \rightarrow 1_{2N}/(2N)$ as $t \rightarrow \infty$, this time almost surely. These two properties put together justify the use of Algorithm 1 in convergence diagnostics: Theorem 1 ensures it provides an upper bound of any f -divergence of the target distribution with respect to the current system of particles and, under ergodicity conditions, this upper bound converges to 0 as $t \rightarrow \infty$. This last statement is proven by the following immediate proposition.

Proposition 1. *Let f define a divergence as in Definition 1. Assume furthermore that f is continuous at 1. If $W_t^{1:N}$ is a random sequence of vectors in $(0, 1)^N$ converging to $1_N/N$ almost surely as $t \rightarrow \infty$, then*

$$\frac{1}{N} \sum_{n=1}^N f(NW_t^n) \rightarrow 0$$

almost surely as well.

Remark 3. All divergences considered in Example 1 are continuous at 1.

Algorithm 1: Weight-harmonization of MCMC simulations

Input: Particles $X_t^{1:2N}$, weights $W_t^{1:2N}$, pairings $A_t^{1:N}$, and coupled kernel \bar{K} .
Output: Updated particles $X_{t+1}^{1:2N}$, weights $W_{t+1}^{1:2N}$, and pairings $A_{t+1}^{1:N}$.

```

2 1. Couple particles and update weights
3  $C \leftarrow \emptyset$ 
   // Collect indices of coupled pairs.
4 for  $n \leftarrow 1$  to  $N$  do
5    $m \leftarrow A_t^n$ 
6   Sample  $(X_{t+1}^n, X_{t+1}^{m+N}) \sim \bar{K}(X_t^n, X_t^{m+N}, \cdot, \cdot)$ 
7   if  $X_{t+1}^n = X_{t+1}^{m+N}$  then
8      $w_* \leftarrow (W_t^n + W_t^{m+N})/2$ 
9      $W_{t+1}^n \leftarrow w_*; W_{t+1}^{m+N} \leftarrow w_*$ 
10     $C \leftarrow C \cup \{n\}$ 
11  else
12     $W_{t+1}^n \leftarrow W_t^n; W_{t+1}^{m+N} \leftarrow W_t^{m+N}$ 
14 2. Reshuffle pairings for the next step
15  $A_{t+1} \leftarrow A_t$ 
16 if  $|C| > 1$  then
17   Sample  $\sigma$ , a uniformly random permutation of the set  $C$  and set  $\sigma(n) = n$  for all  $n \notin C$ 
18   foreach  $n = 1, \dots, N$  do
19      $A_{t+1}^n \leftarrow A_t^{\sigma(n)}$ 

```

4 Theoretical results

4.1 Consistency for a large number of chains

The following proposition shows that Algorithm 1 preserves expectations.

Proposition 2 (Invariance of expectations under Algorithm 1). *Consider the un-normalized estimator $\hat{I}_{t,N}(\varphi) = \sum_{n=1}^{2N} w_t^n \varphi(X_t^n)$ at step t of Algorithm 1, where the w_t^n are the un-normalized weights as per Remark 2. If the Markov kernel K admits π as an invariant distribution, then, for any bounded function φ and for all $t \geq 0$,*

$$E\{\hat{I}_{t,N}(\varphi)\} = E\{\hat{I}_{0,N}(\varphi)\} = 2N \int \varphi(x) \gamma(dx)$$

is constant over time.

In addition to expectations being invariant, the following result states that they are consistent at any iteration of the algorithm.

Theorem 2 (Consistency). *For any initial distribution such that $E_\pi(w_0^2) < \infty$ and function φ such that $E_\pi[\varphi(X)^4] < \infty$, we have*

$$\frac{1}{2N} \sum_{n=1}^{2N} w_t^n \varphi(X_t^n) \rightarrow \int \varphi(x) \gamma(dx), \quad \frac{1}{2N} \sum_{n=1}^{2N} W_t^n \varphi(X_t^n) \rightarrow \int \varphi(x) \pi(dx),$$

where the convergences are in probability.

Describing the exact rate at which the convergence happens for different times t is complex and would depend on the properties of the Markov chain, the coupling, and target distribution. However, it is clear that it cannot worsen as t increases, because, the variance of the weights cannot increase from iteration to iteration of Algorithm 1 as we prove in Section 4.2.

4.2 Geometric weight harmonization under a strong coupling assumption

The previous section proved that, at any iteration of Algorithm 1, our weighted system of particles can be used to form a valid upper bound (10) to the f -divergence $D_f(\pi||\mu_t)$. The following proposition ensures that this bound is furthermore non-increasing.

Proposition 3 (Non-increasing f -divergence bounds). *Let W_t^n be the un-normalized weights at step t of Algorithm 1. For any convex function f , the upper bound (10) verifies*

$$\sum_{n=1}^{2N} f(NW_{t+1}^n) \leq \sum_{n=1}^{2N} f(NW_t^n)$$

almost surely.

Remark 4. This property is an empirical desirable counterpart to the data-processing inequality applied to Markov chains: for any f -divergence D_f , $D_f(\pi||\mu_t)$ must be non-increasing with t (see Theorem 16.1.10 in Cover and Thomas, 2005, for the special case of the KL divergence, the f -divergence case being an immediate generalization).

Taking $f(x) = x^2$, we can immediately deduce that the variance of the weights must decrease too.

Corollary 1 (Non-increasing squared sum of weights). *Let W_t^n be the normalized weights at step t . We have*

$$\sum_{n=1}^{2N} (W_{t+1}^n)^2 \leq \sum_{n=1}^{2N} (W_t^n)^2. \quad (7)$$

If (7) were to hold in a contractive manner: $\sum_{n=1}^{2N} (W_{t+1}^n)^2 < \sum_{n=1}^{2N} (W_t^n)^2$, the only possible fixed point for the system would then be $W_t^n = 1/(2N)$, $n = 1, \dots, 2N$. We now analyse the rate at which the convergence to this fixed point occurs *on average* in terms of the properties of the kernel used.

To do so we use two assumptions, the first one is that σ in Algorithm 1 is taken to be a random permutation of the set of coupled indices. This is not a strict assumption, and the analysis still follows through (at the cost of additional technicalities, e.g., tracking the first time when at least two indices couple) for the more efficient choice of derangements, which we use in Section 5.

Assumption 4 (Uniform Reshuffling). We assume that the reshuffling mechanism for the pairings A_t is a uniform permutation of the indices in C_t .

The second assumption states that the kernels at hand have a positive coupling probability irrespective of the current state.

Assumption 5 (Uniform Coupling). The coupled kernel \bar{K} has a uniform positive probability of coupling, i.e., there exists a constant $p_c > 0$ such that for any states x, y ,

$$\text{pr}(X' = Y' | x, y) \geq p_c,$$

where the probability is taken over $\bar{K}(x, y, dx', dy')$.

Remark 5. More often than not, in the literature on computational couplings, the couplings will instead have properties that relate to their meeting time distribution: for $\tau = \inf\{t \mid X_t = Y_t\}$, geometric or polynomial upper bounds $\text{pr}(\tau > t) \leq C(t)$ are often sufficient for results to follow (see Jacob et al., 2020b; Middleton et al., 2020, for geometric and polynomial tails, respectively). The recurring assumption of sub-exponential tails: $\text{pr}(\tau > t) \leq C \exp(-\delta t)$ is very close to our working assumption, albeit a little weaker. Still, we have found working with these more realistic assumptions too restrictive owing to our handling of N interacting chains, rather than only two.

Under these two assumptions, the following theorem ascertains that the variance of the weights converges to 0 exponentially fast as the number of MCMC iterations increases.

Theorem 3. *Let $W_t = (W_t^1, \dots, W_t^{2N})$ be the vector of weights at iteration t of the weight-harmonization algorithm. Under Assumptions 4 and 5, as $t \rightarrow \infty$, the weight vector W_t converges exponentially fast in mean square to the uniform weight vector $\bar{W} = \{1/(2N), \dots, 1/(2N)\}$, i.e.,*

$$E\left(\|W_t - \bar{W}\|_2^2\right) = O(\rho^{t/2})$$

with $\rho = 1 - p_c^3/4 < 1$.

The following corollary then follows from a classical application of Borel–Cantelli’s lemma and Markov’s inequality (see, e.g. Shiryaev, 1996, Exercise 6.8) to the sequence $\sum_{t \geq 0} \rho^{t/2} = 1/(1 - \sqrt{\rho}) < \infty$.

Corollary 2. *Under the same conditions as Theorem 3, the convergence $W_t \rightarrow \bar{W}$ happens almost surely.*

4.3 From consistency to diagnostics

Combining Theorem 1, Theorem 2, and Theorem 3, we can see that $\sum_{n=1}^N f(NW_t^n)/N$ can be used as an asymptotic, decreasing-to-zero, upper bound for $D_f(\pi||\mu_t)$, where μ_t is the distribution of the MCMC chain at time t . While it is not obvious to express Assumptions 2 and 3 directly in terms of the initial distribution μ_0 and the target distribution π , we point out some important cases in which these conditions are easily verified.

Corollary 3. *Suppose that the weights w_0^n are bounded, i.e. there exists $M < \infty$ such that the Radon–Nikodym derivative $d\pi/d\mu_0$ satisfies $d\pi/d\mu_0 \leq M$ almost surely with respect to μ_0 . Consider an f -divergence such that f is continuously differentiable at 0. Then*

$$\text{pr}\left\{\frac{1}{N} \sum_{n=1}^N f(NW_t^n) \leq D_f(\pi||\mu_t) - \varepsilon\right\} \rightarrow 0.$$

This corollary requires the continuous differentiability of f at time 0 and therefore is not applicable to the Kullback–Leibler divergence. The following result addresses this shortcoming.

Corollary 4. *Let the space be \mathbb{R}^d and suppose that the initial distribution μ_0 and the target distribution π have densities with respect to the Lebesgue measure. Assume that there exist finite M_1 and M_2 such that $\pi(x) \leq M_1 \mu_0(x)$ and $\mu_0(x) \leq M_2$. Suppose further that $E_\pi\{(1 + |\log \pi(X)|)^4\} < \infty$ and that the kernel K is regular in the sense of Appendix H.1. Then*

$$\text{pr}\left\{\frac{1}{N} \sum_{n=1}^N f(NW_t^n) \leq \text{KL}(\pi||\mu_t) - \varepsilon\right\} \rightarrow 0$$

for $f(t) = t \log t$ with the convention that $f(0) = 0$.

In Appendix H.2 we verify the regularity conditions for a random walk Metropolis–Hastings kernel on a Gaussian target distribution.

Remark 6. Corollaries 3 and 4 do not cover the *reversed* KL divergence, given by $f(t) = -\log t$. The derivative magnitude $|f'(t)| = 1/t$ blows up more rapidly at time 0 than what can be compensated by usual moment conditions. This is validated by experiments, see Figure 8.

5 Numerical illustrations

5.1 A fully tractable system

We first turn to a case where all marginal distributions are tractable, and therefore the properties of the proposed method can be assessed without resorting to approximations. When $\mu_0 \sim \mathcal{N}(\mu, \Sigma)$ and $\pi \sim \mathcal{N}(0, I)$ are Gaussian, and under the choice of $K(x, dy) = \mathcal{N}\{y; \rho x, (1 - \rho^2)I\}dy$, for $\rho \in (0, 1)$, we have $\mu_t \sim \mathcal{N}\{\rho^t \mu, \rho^{2t} \Sigma + (1 - \rho^2)I\}$. As a consequence, it is possible to compute $\int (d\pi/d\mu_t) d\pi$ for any $t \geq 0$.

A natural choice of coupling $\tilde{K}(dy', dx' | y, x)$ for K is the *reflection maximal coupling* (see, e.g. Bou-Rabee et al., 2020), which we describe in Appendix I.1. In order to analyse the relative efficiency of our method compared to the real weights, in Figure 2, we report the effective sample size profiles using our method versus the theoretical expected sample size as described in (4) for different values of ρ and N , essentially measuring the gap in Theorem 1. In order to make them comparable, all samplers were rescaled into the same “physical time”: for different ρ , $t \leftarrow t(\log \rho)/(\log \rho_{\max})$.

All experiments target the 100-dimensional standard Gaussian, and start from $\mu_0 \sim \mathcal{N}(10 \cdot 1_{100}, 5 \cdot I_{100})$, largely outside of stationarity. Confidence intervals are shown as two standard deviations for ten independent realizations of Algorithm 1.

A first thing to note: there is no difference in the efficiency that can be attributed to the mixing speed of the kernels: all choices of ρ essentially give the same (after re-scaling) results. Furthermore, small sample-size effects notwithstanding (we can never give an effective sample size smaller than $1/(2N)$), our method is *systematically* conservative in estimating the χ^2 based effective sample size: this is both a feature, as per Theorem 1, and a drawback, as the under estimation does not seem to improve with the mixing of the kernel, and additionally worsens with the number of particles used. Indeed, in the figure, all empirical lines are ordered from left to right in their respective number of particles.

In practice, we conjecture that the empirical effective sample size degradation converges to a non-degenerate “worst case” scenario which still provides useful bounds on the convergence of the system. We come back to this point in Section 6.2 and offer possible avenue for future work easing this problem.

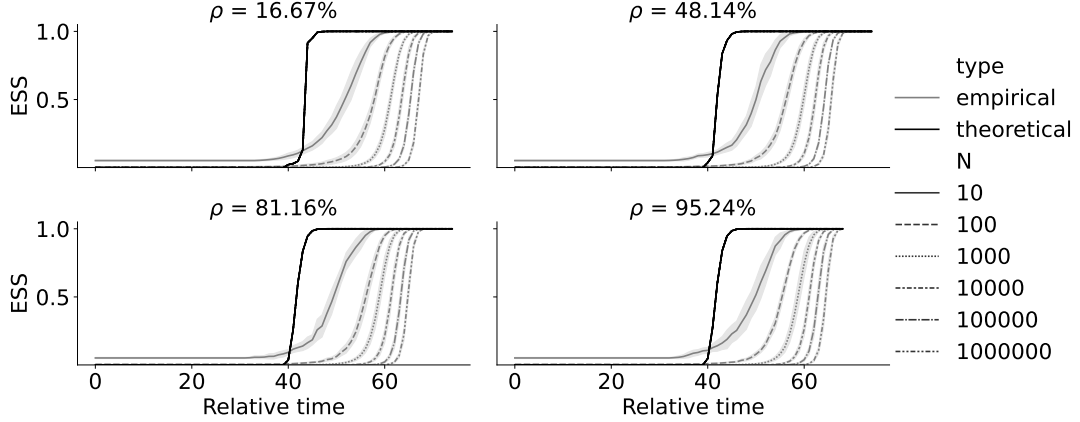


Figure 2: Comparison of theoretical (4) (full, black) and empirical (3) (different dashes correspond to different number of particles, gray) effective sample size measured for μ_t .

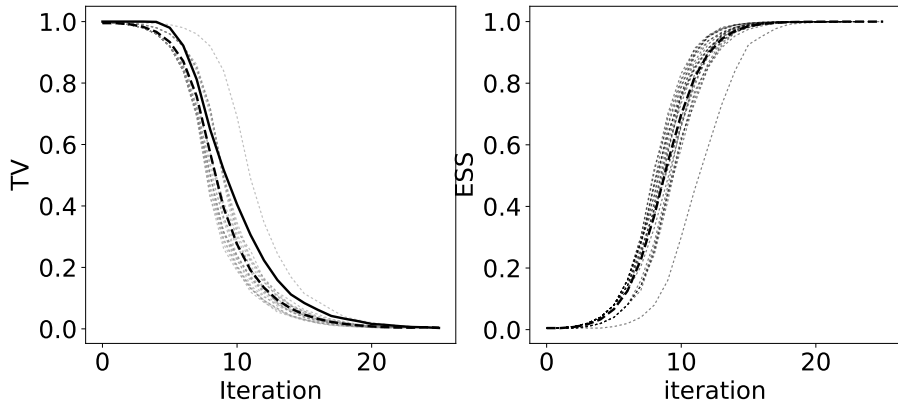


Figure 3: Total variation comparison (left) and ESS (right) profile for the Pólya–Gamma Gibbs sample applied to the Credit dataset logistic regression. Dashed curves correspond to our bound, while the full line corresponds to Biswas et al. (2019).

Other f -divergences profiles are reported in Appendix J: an interesting point to notice therein is that the reverse Kullback–Leibler divergence bounds was largely too conservative and exhibited high variance, which is likely an empirical counterpart to Corollaries 3 and 4 not applying. As a consequence we did not report it there.

5.2 Pólya–Gamma Gibbs sampler for a logistic regression

We now turn to the same real-data example as used by Biswas et al. (2019) for evaluating their total-variation-based convergence diagnostic. The target distribution is defined as a Bayesian logistic regression on the German credit dataset (Hofmann, 1994). It consists of 1000 data entries comprising, after encoding and the addition of an intercept, 49 covariates x_i used to predict the creditworthiness of client i , encoded as an outcome variable $y_i \in \{-1, 1\}$. The model is formally described as $p(y_{1:n}, \beta | x_{1:n}) = \mathcal{N}(\beta; 0_{49}, 10I_{49}) \prod_{i=1}^n (1 + e^{-y_i x_i^\top \beta})$. A powerful MCMC sampler for $p(\beta | y_{1:n}, x_{1:n})$ is the Pólya–Gamma Gibbs sampler (Billingsley, 2012), which performs a Gibbs (Geman and Geman, 1984) routine over an augmented state space. We describe the sampler in Appendix I.4. In order to produce comparable results as Biswas et al. (2019), we use the same coupling strategy, again described in Appendix I.4, and choose the same initial distribution $\mathcal{N}(0, 0_{49}, 10I_{49})$ for all the particles $\beta_0^{1:2N}$ (note the slight change of notations compared to the main text where we used X for the state). We also use the same number of particles $N = 100$ as their number of independent estimators for the total variation between two chains so that we too use $2N = 200$ particles in total. In Figure 3, we report 20 independent realizations of our method and the resulting mean for both the approximate total variation bound and effective sample size profiles. We also reproduce the total variation bound obtained by running the code provided by Biswas et al. (2019) for ease of comparison. Both methods used exactly the same coupling strategy.

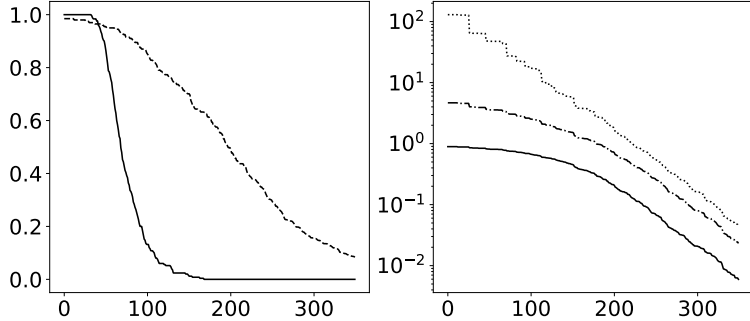


Figure 4: Left: total variation upper bounds of Biswas et al. (2019, full line) and our harmonization procedure (dashed). Right: harmonized upper bounds for the Hellinger distance (full), the KL divergence (dashed) and the χ^2 distance (dotted).

Our method appears to be on par with or better than Biswas et al. (2019) despite not having to implement a pre-run warmup of 350 iterations (in the case of this specific case for Biswas et al., 2019, see Section 3.2). This has to be caveated by a few points however: (i) the two methods do not target exactly the same upper bound to the total variation, and it is not obvious which one would be better, (ii) while Biswas et al. (2019) can only ever improve by increasing the number of estimators (because it is unbiased), we have highlighted in the previous section that our bounds increased with N , (iii) improvements over Biswas et al. (2019) exist: for instance Craiu and Meng (2022) implements control variates to reduce the need for the warm-up, but importantly not changing the eventual bound.

Other f -divergences profiles are reported in Figure 8 in Appendix J.

5.3 MALA for a stochastic volatility model

We now turn to a stochastic volatility model (Liu, 2001, Section 9.6.2) for which we aim to measure the convergence to stationarity of the Metropolis-adjusted Langevin algorithm (Besag, 1994). The model is defined as the distribution

$$\pi(x_{0:L}) \propto \left[\mathcal{N}\{x_0; 0, \sigma^2/(1 - \phi^2)\} \prod_{l=1}^L \mathcal{N}\{x_l; \phi x_{l-1}, \sigma^2\} \right] \times \left[\prod_{l=0}^L \mathcal{N}\{y_l; 0, \beta^2 \exp(x_l)\} \right]$$

over \mathbb{R}^{L+1} for $L = 2499$. In order to proceed with the simulation, we fix the hyper-parameters $(\beta, \phi, \sigma) = (0.65, 0.98, 0.15)$, generate a dataset $y_{0:K}$ as per the model, and use the proposal distribution

$$q(x'_{0:L} | x_{0:L}) = \mathcal{N}\left\{x'_{0:L}; x_{0:L} + \frac{\tau}{2} A \nabla \log \pi(x_{0:L}), \tau A\right\} \quad (8)$$

where A was computed as the covariance corresponding to the Laplace approximation $\mathcal{N}(\mu, A)$ of π , and $\tau = 2.89D^{-1/3}$, which is the optimal value recommended by Roberts and Rosenthal (1998) and corresponds to a 54% acceptance rate in practice, close to the theoretical optimum. We then initialize the particles $X_0^{1:2N}$ from independent draws of $\mathcal{N}(\mu, A)$, and compute the corresponding weights $w_0^n = \pi(X_0^n) / \mathcal{N}(x_0^n; \mu, A)$. The harmonization procedure is then carried using the method in Section 3 for $N = 100$ pairs of chains, and with a maximal reflection coupling of (8), as described in Appendix I.1.

For comparison purposes, we also computed the total variation upper bound of Biswas et al. (2019, see also Section 1) using the same coupling strategy, albeit with a larger number $N = 250$ pairs of chains, owing to some observed variability in the results for lower numbers. The method was used with a warm-up lag of 500 steps, which, based on our harmonization study was largely sufficient to ensure the chains had reached stationarity. We report both of these, together with additional statistics computed by our method, in Figure 4. A key point to note is that, contrary to the results of Section 5.2, we exhibit a more conservative upper bound than Biswas et al. (2019), in particular in the “warm” phase of the algorithm, when the total variation of Biswas et al. (2019) has already started decreasing. This behaviour seems independent of the number of dimensions L and we were able to replicate it for lower values too. We believe this to be a similar occurrence as Section 5.1, where we reach a regime where the harmonization is penalized by its low level of interaction. However, a key point to note is that our procedure, in contrast with Biswas et al. (2019), does not require a warm-up lag to be used. In this specific instance, we can tell *after the fact* that a reasonable lag should have been around or above 200 iterations for this, lower than the 500 steps we used, but it could not have easily been known ahead of time.

6 Discussion

6.1 Summary

We have presented a novel, coupling-based approach to estimating the Radon–Nikodym weights of Markov chain iterates with respect to their target: $(d\mu_t/d\pi)(X_t)$. The procedure, easily implementable as soon as a Markov kernel coupling is available, can be summarized as alternating Markov chain couplings and shufflings to exchange information.

Several properties of the construction have been investigated: first, we (i) have shown consistency at any point in time for increasing number of particles. This is a desirable property that ensures that we can accept the outcome of our algorithm as a trustworthy representation of the target distribution. Second, we (ii) proved that, under assumptions akin to uniform ergodicity, our Radon–Nikodym estimator recovered the expected convergence behaviour: as the number of iteration increases, our weights homogenize towards a common average value and their variance decreases exponentially fast. Finally, based on a novel bound of f -divergences, we (iii) introduced diagnostic criteria for any f -divergence of the system of Markov chains generated with respect to its target distribution. This covered in particular the χ^2 divergence and total variation distance. To the best of our knowledge, our estimator provides the first computable upper bound to f -divergences for Markov chains.

Despite its favourable properties, and competitiveness with alternatives (Section 5.2), our method unfortunately proves conservative when compared to available closed-form solutions (Section 5.1) or on some other benchmarks (Section 5.3). While we believe the method to still be useful *as is*, in the following sections we describe possible future avenues for improvement.

6.2 Perfect sampling example and Rao–Blackwellization

Consider the case when the kernel $K(x, \cdot) = \pi(\cdot)$ produces perfect samples from the target no matter x , in which case, as soon as $t \geq 1$, $d\pi/d\mu_t \equiv 1$ is constant almost everywhere. However, for this ideal scenario, and following Theorem 4, Algorithm 1 will never give better improvements than $\text{ess}_{t+1} \leq \text{ess}_t (1 - \bar{\lambda}/N)^{-N}$, for $\bar{\lambda} = (\kappa_0 - 1)^2/4$ (and $\kappa_0 = \max W_0^{1:2N}/\min W_0^{1:2N}$). For large N , this can be approximated as

$$\text{ess}_{t+1} \lesssim \text{ess}_t \cdot \exp\{\bar{\lambda}\}.$$

This gap, as $N \rightarrow \infty$ can be seen as an asymptotic regime of our method: because $(1 - x/n)^n$ is an increasing function of n for positive x , the achievable improvement has to decrease as $N \rightarrow \infty$ until reaching $\exp\{\bar{\lambda}\}$. We conjecture that this structure holds in general for the expected improvement and general kernels and couplings.

Nonetheless, this sub-efficiency is entirely due to the fact we use pairwise couplings based on the realization of a random permutation. In theory, other pairings could have been chosen, and in this instance, they would all have been successful: when integrating over all possible permutations of $N + 1 : 2N$, for any $m = 1, \dots, 2$, we have

$$E\left(W_1^m \mid W_0^{1:2N}, X_0^{1:2N}\right) = \frac{1}{2N} \sum_{n=1}^N (W_0^m + W_0^{n+N}) = \frac{W_0^m + \frac{1}{N} \sum_{n=1}^N W_0^{n+N}}{2},$$

and similarly for $m = N + 1, \dots, 2N$. These equalities can only be true at the same time if $E\left(W_1^m \mid W_0^{1:2N}, X_0^{1:2N}\right) = 1/(2N)$ for all $m = 1, \dots, 2N$, which would have been the desired result.

This simple analysis offers a first route of improvement for the method: (partial) Rao–Blackwellization over the set of chosen permutations. While this is easy for the simple case highlighted above, doing so for a more general problem is likely harder. Indeed, one would need to keep track of possible coupling trajectories throughout the simulation of the Markov chain, a task that will computationally increase with the number of chains and time steps.

6.3 Forward-coupling, backward-correcting

We have presented an online, single-pass algorithm, where all trajectories are simulated, and past realizations are discarded in computing weights. In some sense, and ignoring the coupling construction, this can be understood as approximating weights functions at time $t + 1$

$$w_{t+1}(x_{t+1}) = \int w_t(x_t) \mu_{t+1}(dx_t \mid x_{t+1})$$

for $\mu_{t+1}(x_t \mid x_{t+1}) \propto \mu_t(x_t) K(x_t, x_{t+1})$, using samples from the prior distribution $X_t^{1:N} \sim \mu_t$. This is similar to approximating smoothing distributions using filtering genealogies in particle filtering (Dau and Chopin, 2023), an approach known to quickly exhibit degeneracy.

This hints at a second route of improvement for the method: if one is willing to perform offline corrections, backward simulation similar to those used in sequential Monte Carlo methods (Chopin and Papaspiliopoulos, 2020) could be used to improve upon the computation of the weights *after an initial pass of our algorithm has been achieved*.

6.4 Control variates and variance reduction

In Craiu and Meng (2022), the authors introduce control variates for the upper bound of Biswas et al. (2019), thereby improving the required “L-lag” warm-up of the method. Such a style of improvement is a likely fruitful research direction for harmonization too: for instance, related but tractable target distributions may be used in a fashion similar to Goodman and Lin (2009), albeit at the cost of implementing a 4-way coupling. The resulting methodology, analysis, and implementation are however not directly obvious and we therefore leave this for future work too.

Acknowledgement

We thank Pierre E. Jacob for providing details on the implementation of the Pólya-Gamma coupled sampler and Yvann Le Fay for saving a factor 2 from being forgotten. AC acknowledges the financial support provided by UKRI for grant EP/Y014650/1, as part of the ERC Synergy project OCEAN. HD would like to acknowledge support from a Singaporean Ministry of Education Tier 2 grant (MOE-T2EP20123-0010).

Supplementary material

The Supplementary Material includes proofs of all results listed in the paper, background on coupling methods for MCMC kernels, as well as additional figures generated for Section 5. Specifically for our main results, Theorem 1 is proven in Appendix B, Theorem 2 is proven in Appendix E, Theorem 3 in Appendix G.

References

Andrieu, C. and Roberts, G. O. (2009). The pseudo-marginal approach for efficient Monte Carlo computations. *The Annals of Statistics*, 37(2):697 – 725.

Besag, J. E. (1994). Contribution to the discussion on ‘Representations of knowledge in complex systems’ by Grenander, U and Miller, M. I.. *Journal of the Royal Statistical Society: Series B (Methodological)*, 56(4):549–581.

Bierkens, J., Fearnhead, P., and Roberts, G. (2019). The Zig-Zag process and super-efficient sampling for Bayesian analysis of big data. *The Annals of Statistics*, 47(3):1288–1320.

Bierkens, J., Grazzi, S., Kamatani, K., and Roberts, G. (2020). The Boomerang Sampler. In III, H. D. and Singh, A., editors, *Proceedings of the 37th International Conference on Machine Learning*, volume 119 of *Proceedings of Machine Learning Research*, pages 908–918. PMLR.

Billingsley, P. (2012). *Probability and Measure*. Wiley Series in Probability and Statistics. Wiley, anniversary edition.

Biswas, N., Bhattacharya, A., Jacob, P. E., and Johndrow, J. E. (2022). Coupling-based convergence assessment of some Gibbs samplers for high-dimensional Bayesian regression with shrinkage priors. *Journal of the Royal Statistical Society: Series B (Statistical Methodology)*, 2.

Biswas, N., Jacob, P. E., and Vanetti, P. (2019). Estimating convergence of Markov chains with L-lag couplings. *Advances in Neural Information Processing Systems*, 32.

Bou-Rabee, N., Eberle, A., and Zimmer, R. (2020). Coupling and convergence for Hamiltonian Monte Carlo. *The Annals of Applied Probability*, 30(3):1209–1250.

Bouchard-Côté, A., Vollmer, S. J., and Doucet, A. (2018). The bouncy particle sampler: A nonreversible rejection-free Markov chain Monte Carlo method. *Journal of the American Statistical Association*, 113(522):855–867.

Brooks, S., Gelman, A., Jones, G., and Meng, X.-L. (2011). *Handbook of Markov chain Monte Carlo*. CRC press.

Ceriani, P. M. and Zanella, G. (2024). Linear-cost unbiased posterior estimates for crossed effects and matrix factorization models via couplings.

Chopin, N. and Papaspiliopoulos, O. (2020). *An Introduction to Sequential Monte Carlo*. Springer.

Corenflos, A., Sutton, M., and Chopin, N. (2025). Debiasing piecewise deterministic markov process samplers using couplings. *Scandinavian Journal of Statistics*, n/a(n/a):1–43.

Cover, T. M. and Thomas, J. A. (2005). *Elements of Information Theory*. John Wiley & Sons, Ltd, USA.

Craiu, R. V. and Meng, X.-L. (2022). Double Happiness: Enhancing the Coupled Gains of L-lag Coupling via Control Variates. *Statistica Sinica*, 32(4):1745–1766.

Dau, H.-D. and Chopin, N. (2023). On backward smoothing algorithms. *The Annals of Statistics*, 51(5):2145 – 2169.

Douc, R., Moulines, E., Priouret, P., and Soulier, P. (2018). *Markov Chains*. Springer International Publishing.

Gelman, A. and Rubin, D. B. (1992). Inference from Iterative Simulation Using Multiple Sequences. *Statistical Science*, 7(4):457 – 472.

Geman, S. and Geman, D. (1984). Stochastic relaxation, Gibbs distributions, and the Bayesian restoration of images. *IEEE Transactions on pattern analysis and machine intelligence*, PAMI-6(6):721–741.

Giles, M. B. (2015). Multilevel Monte Carlo methods. *Acta Numerica*, 24:259–328.

Glynn, P. W. and Rhee, C.-h. (2014). Exact estimation for Markov chain equilibrium expectations. *Journal of Applied Probability*, 51(A):377–389.

Goodman, J. B. and Lin, K. K. (2009). Coupling control variates for Markov chain Monte Carlo. *Journal of Computational Physics*, 228(19):7127–7136.

Heng, J. and Jacob, P. E. (2019). Unbiased Hamiltonian Monte Carlo with couplings. *Biometrika*, 106(2):287–302.

Hofmann, H. (1994). Statlog (German Credit Data). UCI Machine Learning Repository. DOI: <https://doi.org/10.24432/C5NC77>.

Huber, M. L. (2016). *Perfect simulation*, volume 148. CRC Press.

Jacob, P. E., Lindsten, F., and Schön, T. B. (2020a). Smoothing with couplings of conditional particle filters. *Journal of the American Statistical Association*, 115(530):721–729.

Jacob, P. E., O’Leary, J., and Atchadé, Y. F. (2020b). Unbiased Markov chain Monte Carlo methods with couplings. *Journal of the Royal Statistical Society: Series B (Statistical Methodology)*, 82(3):543–600.

Kahn, H. and Harris, T. E. (1951). Estimation of particle transmission by random sampling. *National Bureau of Standards applied mathematics series*, 12:27–30.

Karjalainen, J., Lee, A., Singh, S. S., and Vihola, M. (2023). Mixing time of the conditional backward sampling particle filter. *arXiv preprint arXiv:2312.17572*.

Kong, A., Liu, J. S., and Wong, W. H. (1994). Sequential imputations and Bayesian missing data problems. *Journal of the American Statistical Association*, 89(425):278–288.

Lee, A., Singh, S. S., and Vihola, M. (2020). Coupled conditional backward sampling particle filter. *Annals of Statistics*, 48(5):3066–3089.

Liu, J. S. (2001). *Monte Carlo Strategies in Scientific Computing*. Springer Series in Statistics. Springer.

Metropolis, N., Rosenbluth, A. W., Rosenbluth, M. N., Teller, A. H., and Teller, E. (1953). Equation of state calculations by fast computing machines. *Journal of Chemical Physics*, 21(6):1087–1092.

Meyn, S. P. and Tweedie, R. L. (2009). *Markov chains and stochastic stability*. Cambridge University Press.

Middleton, L., Deligiannidis, G., Doucet, A., and Jacob, P. E. (2019). Unbiased smoothing using particle independent Metropolis-Hastings. In *The 22nd International Conference on Artificial Intelligence and Statistics*, pages 2378–2387. PMLR.

Middleton, L., Deligiannidis, G., Doucet, A., and Jacob, P. E. (2020). Unbiased Markov chain Monte Carlo for intractable target distributions. *Electronic Journal of Statistics*, 14(2):2842–2891.

Neal, R. M. (2011). MCMC using Hamiltonian dynamics. In *Handbook of Markov Chain Monte Carlo*, chapter 5, pages 113–163. Chapman & Hall/CRC.

Nguyen, T. D., Trippe, B. L., and Broderick, T. (2022). Many processors, little time: MCMC for partitions via optimal transport couplings. In *International Conference on Artificial Intelligence and Statistics*, pages 3483–3514. PMLR.

Papp, T. P. and Sherlock, C. (2024). Scalable couplings for the random walk metropolis algorithm. *Journal of the Royal Statistical Society Series B: Statistical Methodology*, page qkae113.

Peyré, G. and Cuturi, M. (2019). Computational Optimal Transport: With Applications to Data Science. *Foundations and Trends in Machine Learning*, 11(5-6):355–607.

Polson, N. G., Scott, J. G., and Windle, J. (2013). Bayesian inference for logistic models using pólya–gamma latent variables. *Journal of the American Statistical Association*, 108(504):1339–1349.

Propp, J. G. and Wilson, D. B. (1996). Exact sampling with coupled Markov chains and applications to statistical mechanics. *Random Structures & Algorithms*, 9(1-2):223–252.

Rényi, A. (1961). On measures of entropy and information. In *Proceedings of the Fourth Berkeley Symposium on Mathematical Statistics and Probability, Volume 1: Contributions to the Theory of Statistics*, volume 4, pages 547–562. University of California Press.

Rhee, C.-H. and Glynn, P. W. (2015). Unbiased estimation with square root convergence for SDE models. *Operations Research*, 63(5):1026–1043.

Roberts, G. O. and Rosenthal, J. S. (1998). Optimal scaling of discrete approximations to Langevin diffusions. *Journal of the Royal Statistical Society: Series B (Statistical Methodology)*, 60(1):255–268.

Shiryayev, A. N. (1996). *Probability*. Springer, 2nd edition.

Uhlenbeck, G. E. and Ornstein, L. S. (1930). On the theory of the Brownian motion. *Phys. Rev.*, 36:823–841.

Vats, D. and Knudson, C. (2021). Revisiting the Gelman–Rubin Diagnostic. *Statistical Science*, 36(4):518 – 529.

Vehtari, A., Gelman, A., Simpson, D., Carpenter, B., and Bürkner, P.-C. (2021). Rank-Normalization, Folding, and Localization: An Improved \widehat{R} for Assessing Convergence of MCMC (with Discussion). *Bayesian Analysis*, 16(2):667 – 718.

Vihola, M. (2018). Unbiased estimators and multilevel Monte Carlo. *Operations Research*, 66(2):448–462.

Villani, C. (2009). *Optimal transport: old and new*, volume 338. Springer.

Wang, G., O’Leary, J., and Jacob, P. (2021). Maximal couplings of the metropolis-hastings algorithm. In Banerjee, A. and Fukumizu, K., editors, *Proceedings of The 24th International Conference on Artificial Intelligence and Statistics*, volume 130 of *Proceedings of Machine Learning Research*, pages 1225–1233. PMLR.

A Notations for the proofs

We write \mathcal{F}_t be the filtration generated by all particles, weights, and pairings up to time t . When a particle X_t^n is associated with a particle $X^{A_t^n+N}$, we write $m_t^n = A_t^n + N$ for short, dropping the t index when context is clear.

B Proof of Theorem 1

The following lemma is standard but useful to cover the case of the total variation for which $f(t) = |t - 1|/2$.

Lemma 2. *Suppose that the function f satisfies Assumption 1, and that there exists a point $0 < c < \infty$ such that f is continuously differentiable on $(0, c)$ and (c, ∞) . Then*

$$-\infty < \lim_{t \rightarrow c^-} f'(t) \leq \lim_{t \rightarrow c^+} f'(t) < \infty$$

and the convention

$$f'(c) = \frac{1}{2} \left\{ \lim_{t \rightarrow c^-} f'(t) + \lim_{t \rightarrow c^+} f'(t) \right\}$$

is well defined. Moreover the identity

$$f(x) \geq f(y) + f'(y)(x - y)$$

still holds for all pairs (x, y) , including when one of the entries is equal to c or the two entries are on different sides of c .

Proof. Because f is convex, it has a subdifferential at all points, and the subdifferential is a convex set. As a consequence, $f'(c)$ belong to the subdifferential of f at c , even for the case when only a left and right limit exist. The rest follows from the fact that convex functions are lower bounded by their tangents. \square

Proof of Theorem 1. The proof relies on the convexity of the function f that defines the divergence. Let $Q_N = \sum_{n=1}^N f(NW^n)/N$ be our estimator. We have

$$\begin{aligned} Q_N - D_f(\pi || \mu) &= \frac{1}{N} \sum_{n=1}^N f(NW^n) - \int f(\psi(x)) \mu(dx) \\ &= \left[\frac{1}{N} \sum_{n=1}^N (f(NW^n) - f\{\psi(X^n)\}) \right] + \left[\frac{1}{N} \sum_{n=1}^N f\{\psi(X^n)\} - \int f\{\psi(x)\} \mu(dx) \right] \end{aligned} \quad (9)$$

Owing to the convexity and differentiability of f , the first term in (9) can be bounded from below:

$$\begin{aligned} \frac{1}{N} \sum_{n=1}^N (f(NW^n) - f\{\psi(X^n)\}) &\geq \frac{1}{N} \sum_{n=1}^N f'\{\psi(X^n)\} \{NW^n - \psi(X^n)\} \\ &= \left[\sum_{n=1}^N W^n f'\{\psi(X^n)\} \right] - \left[\frac{1}{N} \sum_{n=1}^N \psi(X^n) f'\{\psi(X^n)\} \right] \end{aligned}$$

Let us denote the two terms on the right-hand side as A_N and B_N respectively. By Assumption 2, $A_N \rightarrow \int f'\{\psi(x)\} \pi(dx)$ in probability. By Assumption 3, $B_N \rightarrow \int \psi(x) f'\{\psi(x)\} \mu(dx)$ in probability.

Since $\pi(dx) = \psi(x) \mu(dx)$, the limits are identical:

$$\int f'\{\psi(x)\} \pi(dx) = \int f'\{\psi(x)\} \psi(x) \mu(dx).$$

Therefore, the difference $A_N - B_N \rightarrow 0$ in probability.

Now consider the second term in (9) and call it C_N :

$$C_N = \frac{1}{N} \sum_{n=1}^N f\{\psi(X^n)\} - \int f\{\psi(x)\} \mu(dx).$$

By Assumption 3, $C_N \rightarrow 0$ in probability.

Combining these results, we have a lower bound for the total expression:

$$Q_N - D_f(\pi || \mu) \geq (A_N - B_N) + C_N.$$

Let $L_N = (A_N - B_N) + C_N$. Since $A_N - B_N \rightarrow 0$ in probability and $C_N \rightarrow 0$ in probability, their sum L_N also converges to 0 in probability.

This means that for any $\varepsilon > 0$, $\text{pr}(|L_N| \geq \varepsilon/2) \rightarrow 0$. The event $\{Q_N - D_f(\pi || \mu) \leq -\varepsilon\}$ is a subset of the event $\{L_N \leq -\varepsilon\}$, because $Q_N - D_f(\pi || \mu) \geq L_N$. Thus,

$$\text{pr}\{Q_N - D_f(\pi || \mu) \leq -\varepsilon\} \leq \text{pr}\{L_N \leq -\varepsilon\}.$$

The event $\{L_N \leq -\varepsilon\}$ is itself a subset of $\{|L_N| \geq \varepsilon\}$. Therefore,

$$\text{pr}\{Q_N - D_f(\pi || \mu) \leq -\varepsilon\} \leq \text{pr}\{|L_N| \geq \varepsilon\}.$$

Since $L_N \rightarrow 0$ in probability, the right-hand side tends to 0 as $N \rightarrow \infty$. \square

C Maximum bound on ESS improvement

Theorem 4. Let $W^{1:2N}$ be a set of positive weights, and, for some $j \in \{1, \dots, N\}$, let $\tilde{W}^{1:2N}$ be defined as $\tilde{W}^n = W^n$, $n \in \{1, \dots, 2N\} \setminus \{j, j+N\}$, and $\tilde{W}^j = \tilde{W}^{j+N} = (W^j + W^{j+N})/2$. Then, we have

$$\text{ESS}(\tilde{W}^{1:2N}) = \text{ESS}(W^{1:2N}) \frac{1}{1 - \text{ESS}(W^{1:2N}) \frac{(W^j - W^{j+N})^2}{2}}$$

in particular,

$$\text{ESS}(W^{1:2N}) \leq \text{ESS}(\tilde{W}^{1:2N}) \leq 2\text{ESS}(W^{1:2N})$$

and the left inequality is strict if $W^j \neq W^{j+N}$. Additionally, writing $W_* = \min W^{1:2N}$ and $W^* = \max W^{1:2N}$, and $\kappa = W^*/W_*$, we have the tighter upper bound

$$\text{ESS}(\tilde{W}^{1:2N}) \leq \text{ESS}(W^{1:2N}) \frac{1}{1 - \frac{(\kappa-1)^2}{2(\kappa^2+2N-1)}}. \quad (10)$$

Finally, $\tilde{W}_* \geq W_*$ and the inequality is strict if $W_* \in \{W^j, W^{j+N}\}$ is uniquely represented in $W^{1:2N}$. The same holds in reverse for W^* and \tilde{W}^* and therefore $\tilde{\kappa} = \tilde{W}^*/\tilde{W}_* \leq \kappa$, with a strict inequality under the same conditions.

Remark 7. Using the same lines, it can be shown that $\alpha = 1/2$ maximizes the improvement because, for a general α , it is then

$$\text{ESS}(\tilde{W}^{1:2N}) = \text{ESS}(W^{1:2N}) \frac{1}{1 - \text{ESS}(W^{1:2N}) \frac{\alpha(1-\alpha)(W^j - W^{j+N})^2}{4N}}.$$

Proof. The proof follows from direct computation:

$$\begin{aligned} \sum_{n=1}^{2N} (\tilde{W}^n)^2 &= \sum_{n=1, n \neq j}^N (W^n)^2 + \sum_{n=1, n \neq j}^N (W^{n+N})^2 + 2 \frac{(W^j + W^{j+N})^2}{4} \\ &= \sum_{n=1, n \neq j}^N (W^n)^2 + \sum_{n=1, n \neq j}^N (W^{n+N})^2 + \frac{(W^j)^2 + (W^{j+N})^2 + 2W^j W^{j+N}}{2} \\ &= \sum_{n=1}^{2N} (W^n)^2 - \frac{(W^j - W^{j+N})^2}{2}. \end{aligned}$$

Hence, we have

$$\begin{aligned} \text{ESS}(\tilde{W}^{1:2N}) &= \frac{1}{\sum_{n=1}^{2N} (\tilde{W}^n)^2} = \frac{1}{\sum_{n=1}^{2N} (W^n)^2 - \frac{(W^j - W^{j+N})^2}{2}} \\ &= \text{ESS}(W^{1:2N}) \frac{1}{1 - \frac{(W^j - W^{j+N})^2}{2 \sum_{n=1}^{2N} (W^n)^2}}, \end{aligned}$$

this gives the first equality. Because $(W^j - W^{j+N})^2 \geq 0$, it is clear that $\text{ESS}(W^{1:2N}) \leq \text{ESS}(\tilde{W}^{1:2N})$. For the second inequality,

$$\frac{(W^j - W^{j+N})^2}{2 \sum_{n=1}^{2N} (W^n)^2} \leq \frac{(W^j)^2 + (W^{j+N})^2}{2 \sum_{n=1}^{2N} (W^n)^2} \leq 1/2,$$

so that

$$\frac{1}{1 - \frac{(W^j - W^{j+N})^2}{2 \sum_{n=1}^{2N} (W^n)^2}} \leq \frac{1}{1 - 1/2} = 2.$$

Now, writing $W_* = \min W^{1:2N}$ and $W^* = \max W^{1:2N}$, we have $(W^j - W^{j+N})^2 \leq (W^* - W_*)^2$ so that

$$\frac{(W^j - W^{j+N})^2}{2 \sum_{n=1}^{2N} (W^n)^2} \leq \frac{(W^* - W_*)^2}{2((W^*)^2 + (2N-1)W_*^2)}$$

and the second upper bound follows from reordering the terms. The last two statements are immediate from the definition of \tilde{W} . \square

D Proof of Proposition 2

The proof follows from induction. The base case $t = 0$ is immediate by definition. We first compute the conditional expectation of the sum of un-normalized estimators, $\sum_{i=1}^{2N} w_{t+1}^i \varphi(X_{t+1}^i)$, given the history \mathcal{F}_t . The sum can be grouped into N pairs (n, m^n) that are conditionally independent given \mathcal{F}_t . For one such pair, let $(X', Y') \sim \bar{K}(X_t^n, X_t^{m^n}, \cdot, \cdot)$. The expected contribution of this pair to the sum at time $t + 1$ is

$$E \left[w_{t+1}^n \varphi(X') + w_{t+1}^{m^n} \varphi(Y') \mid \mathcal{F}_t \right].$$

The weight update rule states that if $X' = Y'$, then $w_{t+1}^n = w_{t+1}^{m^n} = (w_t^n + w_t^{m^n})/2$, otherwise the weights are unchanged. The expectation can be written as an integral over the coupled kernel:

$$\int \left[\mathbb{1}(x' = y') \frac{w_t^n + w_t^{m^n}}{2} (\varphi(x') + \varphi(y')) + \mathbb{1}(x' \neq y') \left(w_t^n \varphi(x') + w_t^{m^n} \varphi(y') \right) \right] \bar{K}(X_t^n, X_t^{m^n}, dx', dy').$$

On the event $x' = y'$, the first term is $(w_t^n + w_t^{m^n})\varphi(x')$. We can rewrite the integral as

$$\begin{aligned} & \int \left(w_t^n \varphi(x') + w_t^{m^n} \varphi(y') \right) \bar{K}(\dots, dx', dy') \\ & + \int_{x' \neq y'} \left[(w_t^n + w_t^{m^n})\varphi(x') - \left(w_t^n \varphi(x') + w_t^{m^n} \varphi(x') \right) \right] \bar{K}(\dots, dx', dy'). \end{aligned}$$

The second integral is zero. The first integral, by the marginal properties of the coupling \bar{K} , is

$$w_t^n \int \varphi(x') K(X_t^n, dx') + w_t^{m^n} \int \varphi(y') K(X_t^{m^n}, dy') = w_t^n (K\varphi)(X_t^n) + w_t^{m^n} (K\varphi)(X_t^{m^n}).$$

Summing over all pairs $n = 1, \dots, N$ and taking the total expectation gives

$$E[\hat{I}_{t+1, N}(\varphi)] = E \left[\frac{1}{2N} \sum_{i=1}^{2N} w_t^i (K\varphi)(X_t^i) \right] = E[\hat{I}_{t, N}(K\varphi)].$$

For the inductive step, assume $E[\hat{I}_{t, N}(\psi)] = \pi(\psi)$ for any bounded function ψ . Then

$$E[\hat{I}_{t+1, N}(\varphi)] = E[\hat{I}_{t, N}(K\varphi)].$$

Applying the inductive hypothesis with $\psi = K\varphi$ gives $E[\hat{I}_{t, N}(K\varphi)] = \pi(K\varphi)$. Since π is an invariant distribution for K ,

$$\pi(K\varphi) = \int (K\varphi)(x) \pi(dx) = \int \varphi(x) (\pi K)(dx) = \int \varphi(x) \pi(dx) = \pi(\varphi).$$

E Proof of Theorem 2

Lemma 3. *For any $\alpha \geq 1$ and any π -invariant kernel K , if $E_\pi\{\varphi(X)^\alpha\} < \infty$ then $E_\pi[\{(K\varphi)(X)\}^\alpha] < \infty$.*

Proof. By Jensen's inequality

$$E_\pi[\{(K\varphi)(X)\}^\alpha] = \int \left\{ \int \varphi(y) K(x, dy) \right\}^\alpha \pi(dx) \leq \iint \varphi(y)^\alpha K(x, dy) \pi(dx).$$

The π -invariance of the kernel then concludes the proof. \square

Lemma 4. *For any non-negative function φ , we have*

$$E \left\{ \sum_{n=1}^{2N} (w_t^n)^2 \varphi(X_t^n) \right\} \leq E \left\{ \sum_{n=1}^{2N} (w_{t-1}^n)^2 (K\varphi)(X_{t-1}^n) \right\}.$$

Proof. Write

$$\begin{aligned} \sum_{n=1}^{2N} (w_t^n)^2 \varphi(X_t^n) &= \sum_{n=1}^N (w_t^n)^2 \varphi(X_t^n) + (w_t^{m_{t-1}^n})^2 \varphi(X_t^{m_{t-1}^n}) \\ &\leq \sum_{n=1}^N (w_{t-1}^n)^2 \varphi(X_t^n) + (w_{t-1}^{m_{t-1}^n})^2 \varphi(X_t^{m_{t-1}^n}) \end{aligned}$$

where the inequality ‘ \leq ’ holds for each individual term of the summation thanks to the coupling mechanism. The proof is concluded by taking the expectation on both sides. \square

Proof of Theorem 2. We prove that statement by induction on t . We first remark that

$$\begin{aligned} \hat{\theta}_t &= \frac{1}{2N} \sum_{n=1}^{2N} w_t^n \varphi(X_t^n) = \frac{1}{2N} \sum_{n=1}^N w_t^n \varphi(X_t^n) + w_t^{m_{t-1}^n} \varphi(X_t^{m_{t-1}^n}) \\ &= \frac{1}{2N} \sum_{n=1}^N w_{t-1}^n \varphi(X_t^n) + w_{t-1}^{m_{t-1}^n} \varphi(X_t^{m_{t-1}^n}) \end{aligned}$$

where the equality holds for each individual term in the summation thanks to the weight harmonization mechanism. Remark that

$$\begin{aligned} E \left\{ \frac{1}{2N} \sum_{n=1}^{2N} w_t^n \varphi(X_t^n) \mid \mathcal{F}_{t-1} \right\} &= \frac{1}{2N} \sum_{n=1}^N w_{t-1}^n K \varphi(X_{t-1}^n) + w_{t-1}^{m_{t-1}^n} K \varphi(X_{t-1}^{m_{t-1}^n}) \\ &= \theta_{t-1} \end{aligned}$$

where \mathcal{F}_{t-1} contains all variables up to time $t-1$ included, *including* the shuffling. Now, $\theta_{t-1} \xrightarrow{\text{pr}} \int (K\varphi) d\gamma = \int \varphi d\gamma$ by induction hypothesis (Note the subtle use of Lemma 3 to make sure that the fourth moment condition also holds for $K\varphi$ instead of φ). Thus we only need to show that

$$\hat{\theta}_t - \theta_{t-1} \rightarrow 0$$

in probability. Using Chebyshev’s inequality

$$\begin{aligned} \text{pr}(\hat{\theta}_t - \theta_{t-1} \geq \varepsilon \mid \mathcal{F}_{t-1}) &\leq \varepsilon^{-2} E \left\{ (\hat{\theta}_t - \theta_{t-1})^2 \mid \mathcal{F}_{t-1} \right\} \\ &= \varepsilon^{-2} \text{Var} \left(\frac{1}{2N} \sum_{n=1}^N w_{t-1}^n \varphi(X_t^n) + w_{t-1}^{m_{t-1}^n} \varphi(X_t^{m_{t-1}^n}) \mid \mathcal{F}_{t-1} \right) \\ &= (2\varepsilon N)^{-2} \sum_{n=1}^N \text{Var}(w_{t-1}^n \varphi(X_t^n) + w_{t-1}^{m_{t-1}^n} \varphi(X_t^{m_{t-1}^n}) \mid \mathcal{F}_{t-1}) \\ &\leq \frac{1}{2} (\varepsilon N)^{-2} \sum_{n=1}^N (w_{t-1}^n)^2 (K[\varphi^2])(X_{t-1}^n) + (w_{t-1}^{m_{t-1}^n})^2 (K[\varphi^2])(X_{t-1}^{m_{t-1}^n}) \\ &= \frac{1}{2\varepsilon^2 N^2} \sum_{n=1}^{2N} (w_{t-1}^n)^2 (K[\varphi^2])(X_{t-1}^n). \end{aligned}$$

Now taking expectation of both sides and applying Lemma 4 repeatedly, we have

$$\text{pr}(\hat{\theta}_t - \theta_{t-1} \geq \varepsilon) \leq \frac{1}{\varepsilon^2 N} E[(w_0^1)^2 K^t[\varphi^2](X_0^1)]. \quad (11)$$

Now the last expectation does not depend on N , so to prove that (11) converges to 0 as $N \rightarrow \infty$ it remains to check that that expectation is finite. We have

$$E\{(w_0^1)^2 K^t(\varphi^2)(X_0^1)\} = E_\pi\{w_0(X) K^t(\varphi^2)(X)\} \leq (E_\pi[w_0^2] E_\pi\{|K^t(\varphi^2)|\}^2)^{1/2}$$

using Cauchy–Schwarz’s inequality. The first expectation is finite by assumption. The second is finite too given that $E_\pi[\varphi^4] < \infty$ and Lemma 3 with $\alpha = 2$ and kernel K^t . \square

F Proof of Proposition 3

Consider the f -divergence upper bound at time t :

$$\sum_{n=1}^{2N} f(NW_t^n).$$

The weight update only affects pairs of particles that couple. We first analyze the effect on a single pair $(n, m^n = A_t^n + N)$. The weights before the update are W_t^n and $W_t^{m^n}$.

- If the particles do not couple, $W_{t+1}^n = W_t^n$ and $W_{t+1}^{m^n} = W_t^{m^n}$. The contribution to the upper bound, $f(NW_t^n) + f(NW_t^{m^n})$, is unchanged.
- If the particles do couple, the new weights become $W_{t+1}^n = W_{t+1}^{m^n} = (W_t^n + W_t^{m^n})/2$. By convexity of f , using Jensen's inequality, the contribution to the upper bound is *decreased*

$$f(NW_{t+1}^n) + f(NW_{t+1}^{m^n}) \leq f(NW_t^n) + f(NW_t^{m^n}).$$

In either case, for any realization of the algorithm and for any pair, the contribution to the f -divergence bound is non-increasing. Summing over all pairs, we have for any realization:

$$\sum_{n=1}^{2N} f(NW_{t+1}^n) \leq \sum_{n=1}^{2N} f(NW_t^n).$$

G Proof of Theorem 3

The core idea is to show that the expected squared Euclidean distance to the uniform weight vector \bar{W} is a Lyapunov function for the process, contracting every two steps. Let $V_t = \|W_t - \bar{W}\|_2^2 = \sum_{i=1}^{2N} \{W_t^i - 1/(2N)\}^2$. Note that $V_t = 0$ if and only if $W_t = \bar{W}$.

We start by stating two easily verified identities: for any collection of real numbers $(q_n)_{n=1}^N$,

$$\sum_{n=1}^N (q_n - \bar{q})^2 = \frac{1}{2N} \sum_{m,n=1}^N (q_n - q_m)^2 \quad (12)$$

with $\bar{q} = \sum_{n=1}^N q_n/N$, and for any $x, y, z \in \mathbb{R}$,

$$(x - y)^2 + (x + y - 2z)^2 = 2[(x - z)^2 + (y - z)^2]. \quad (13)$$

Now, at each step $t + 1$, for each pair of indices (n, m_t^n) where $m_t^n = A_t^n + N$, the particles are propagated through the coupled kernel \bar{K} . If the particles couple, which occurs with probability $p_{n,t} \geq p_c$, their corresponding weights are averaged: $W_{t+1}^n = W_{t+1}^{m_t^n} = (W_t^n + W_t^{m_t^n})/2$. If they do not couple, the weights remain unchanged.

The weight update rule implies that the sum of weights is conserved, $\sum_{i=1}^{2N} W_{t+1}^i = \sum_{i=1}^{2N} W_t^i = 1$.

We can express V_{t+1} in terms of V_t . The change in the sum of squares only affects the weights of coupled pairs. Let C_{t+1} be the random set of indices $n \in \{1, \dots, N\}$ for which the corresponding pair of particles coupled at step $t + 1$. For a single coupled pair indexed by $n \in C_{t+1}$ (with partner $m_t^n = A_t^n + N$), the change in their contribution to V_t is:

$$\begin{aligned} \Delta V_n &= 2 \left(\frac{W_t^n + W_t^{m_t^n}}{2} - \frac{1}{2N} \right)^2 - \left(W_t^n - \frac{1}{2N} \right)^2 - \left(W_t^{m_t^n} - \frac{1}{2N} \right)^2 \\ &= -\frac{1}{2} (W_t^n - W_t^{m_t^n})^2, \end{aligned}$$

as per the second identity (13) stated at the beginning of this proof. Summing over all coupled pairs, we get the total change in V_t :

$$V_{t+1} = V_t + \sum_{n \in C_{t+1}} \Delta V_n = V_t - \frac{1}{2} \sum_{n \in C_{t+1}} \left(W_t^n - W_t^{m_t^n} \right)^2.$$

Now, let \mathcal{F}_t be the filtration generated by the history of particles and pairings up to time t . We take the conditional expectation with respect to the random coupling events.

$$\begin{aligned} E[V_{t+1} | \mathcal{F}_t] &= E\left[V_t - \frac{1}{2} \sum_{n=1}^N \mathbb{1}\{n \in C_{t+1}\} (W_t^n - W_t^{m_t^n})^2 | \mathcal{F}_t\right] \\ &= V_t - \frac{1}{2} \sum_{n=1}^N E[\mathbb{1}\{n \in C_{t+1}\} | \mathcal{F}_t] (W_t^n - W_t^{m_t^n})^2. \end{aligned} \quad (14)$$

By Assumption 5, the probability that pair n couples is at least p_c , regardless of the current particle states $X_t^n, X_t^{m_t^n}$. Thus, $E[\mathbb{1}\{n \in C_{t+1}\} | \mathcal{F}_t] \geq p_c$. This gives us:

$$E[V_{t+1} | \mathcal{F}_t] \leq V_t - \frac{p_c}{2} \sum_{n=1}^N (W_t^n - W_t^{m_t^n})^2.$$

The term $\sum_{n=1}^N (W_t^n - W_t^{m_t^n})^2$ represents the potential for variance reduction for a given pairing A_t .

Applying the same argument to $E[V_t | \mathcal{F}_{t-1}] \leq V_{t-1} - p_c \sum_{n=1}^N (W_{t-1}^n - W_{t-1}^{m_{t-1}^n})^2 / 2$, we can then write, using the tower law of expectations, that, conditionally on all random variables generated up to time $t-1$,

$$E[V_{t+1} | \mathcal{F}_{t-1}] \leq V_{t-1} - \frac{p_c}{2} \sum_{n=1}^N (W_{t-1}^n - W_{t-1}^{m_t^n})^2 - \frac{p_c}{2} E\left[\sum_{n=1}^N (W_t^n - W_t^{m_t^n})^2 | \mathcal{F}_{t-1}\right].$$

Now, one can show by rearranging terms, that because $(A_t^n)_{n=1}^N$ is a uniform shuffling of $(A_{t-1}^n)_{n=1}^N$ (as per Assumption 4) on C_t

$$E\left[\sum_{n=1}^N (W_t^n - W_t^{m_t^n})^2 | \mathcal{F}_{t-1}\right] \geq E\left[\sum_{i,j \in C_t} \frac{1}{|C_t|} (W_t^i - W_t^{m_{t-1}^j})^2 | \mathcal{F}_{t-1}\right]$$

where, by convention $0/0 = 0$ and empty sums are null so that the inequality is trivial if no coupling happens. As a consequence, using the definition of W_t^n as an average of W_{t-1}^n and $W_{t-1}^{m_{t-1}^n}$ as well as using (12) stated at the beginning of this proof, the above inequality implies

$$\begin{aligned} E\left[\sum_{n=1}^N (W_t^n - W_t^{m_t^n})^2 | \mathcal{F}_{t-1}\right] &\geq \frac{1}{4} E\left[\sum_{i,j \in C_t} \frac{1}{|C_t|} \left(W_{t-1}^i + W_{t-1}^{m_t^i} - W_{t-1}^j - W_{t-1}^{m_t^j}\right)^2 | \mathcal{F}_{t-1}\right] \\ &\geq \frac{1}{4N} p_c^2 \sum_{i,j=1}^N \left(W_{t-1}^i + W_{t-1}^{m_t^i} - W_{t-1}^j - W_{t-1}^{m_t^j}\right)^2 \end{aligned}$$

where we have used the fact that $|C_t| \leq N$, and the same inequality of the sum on C_t as in (14). Finally, using (12)

$$E\left[\sum_{n=1}^N (W_t^n - W_t^{m_t^n})^2 | \mathcal{F}_{t-1}\right] \geq \frac{p_c^2}{2} \sum_{n=1}^N \left(W_{t-1}^n + W_{t-1}^{m_t^n} - \frac{1}{N}\right)^2$$

and combining everything, noting that $p_c/2 > p_c^3/4$,

$$\begin{aligned} E[V_{t+1} | \mathcal{F}_{t-1}] &\leq V_{t-1} - \frac{p_c}{2} \sum_{n=1}^N (W_{t-1}^n - W_{t-1}^{m_t^n})^2 - \frac{p_c}{2} E\left[\sum_{n=1}^N (W_t^n - W_t^{m_t^n})^2 | \mathcal{F}_{t-1}\right] \\ &\leq V_{t-1} - \frac{p_c}{2} \sum_{n=1}^N (W_{t-1}^n - W_{t-1}^{m_t^n})^2 - \frac{p_c^3}{4} \sum_{n=1}^N \left(W_{t-1}^n + W_{t-1}^{m_t^n} - \frac{1}{N}\right)^2 \\ &\leq V_{t-1} - \frac{p_c^3}{4} \sum_{n=1}^N (W_{t-1}^n - W_{t-1}^{m_t^n})^2 + \left(W_{t-1}^n + W_{t-1}^{m_t^n} - \frac{1}{N}\right)^2 \\ &= V_{t-1} - \frac{p_c^3}{4} \sum_{n=1}^N (W_{t-1}^n - \frac{1}{2N})^2 + \left(W_{t-1}^n \frac{1}{2N}\right)^2 \\ &= \left(1 - \frac{p_c^3}{4}\right) V_{t-1}. \end{aligned}$$

where the penultimate equality comes from (13) and the last one from the definition of V_{t-1} .

The result then follows from the tower law, starting the recursion either at $E(V_1)$ for odd t 's or $E(V_0)$ for even ones.

H From consistency to diagnostics

H.1 Regular Markov kernels

Definition 2. Let $K(x, dy)$ be a Markov kernel from \mathbb{R}^d to \mathbb{R}^d such that $K(x, dy)$ admits a density with respect to the Lebesgue measure. We define

$$\|K\|_\infty = \sup_{\mu} \frac{\|\mu K\|_\infty}{\|\mu\|_\infty}$$

where the supremum is taken over all densities μ in \mathbb{R}^d for which we define $\|\mu\|_\infty = \sup_{x \in \mathbb{R}^d} \mu(x)$, and the density μK is given by $(\mu K)(x) = \int \mu(y) K(x, y) dy$.

We are now ready to define the notion of regular Markov kernels.

Definition 3. A Markov kernel from \mathbb{R}^d to \mathbb{R}^d admitting a density with respect to the Lebesgue measure is called *regular* if $\|K\|_\infty < \infty$ where $\|K\|_\infty$ is defined in 2.

H.2 Regularity conditions for Corollary 4

In this section we verify the regularity conditions of Corollary 4 for the random walk Metropolis–Hastings algorithm on a Gaussian target distribution π and Gaussian starting distributions μ_0 . The arguments can be easily generalized to larger classes of distributions. The only non-trivial point is the regularity of the Metropolis–Hastings kernel in the sense of Definition 3. Given the current state y , the random walk Metropolis–Hastings algorithm proposes a new state using a proposal $q(dy^*|y)$ of the form

$$q(y^*|y) = \mathcal{N}(y^*; y, \delta \Sigma)$$

for some covariance matrix Σ and a scale parameter δ . The next state is accepted with probability

$$\alpha(y, y^*) = 1 \wedge \frac{\pi(y^*)}{\pi(y)}.$$

The average rejection rate is given by

$$\bar{r}(y) = \int q(y^*|y)(1 - \alpha(y, y^*)) dy$$

so the full kernel reads

$$K(y, dy^*) = q(dy^*|y)\alpha(y, y^*) + r(y)\delta_y(dy^*).$$

Starting from a measure μ , after one iteration the chain has distribution

$$(\mu K)(x) = \int \mu(y) K(y, x) dy = \int \mu(y) q(x|y) \alpha(y, x) dy + r(x)\mu(x).$$

Thus, using the fact that $r(x)$ and $\alpha(y, x)$ are bounded by 1 and the symmetric form of the proposal q ,

$$\begin{aligned} (\mu K)(x) &\leq \int \mu(y) q(x|y) dy + \mu(x) \\ &\leq \|\mu\|_\infty \int q(x|y) dy + \|\mu\|_\infty = \|\mu\|_\infty \int q(y|x) dy + \|\mu\|_\infty \\ &= 2\|\mu\|_\infty. \end{aligned}$$

Thus the kernel K is regular with $\|K\|_\infty \leq 2$.

H.3 Proof of Corollaries 3 and 4

Lemma 5. Suppose that the initial distribution μ_0 and the target distribution π are such that $d\pi/d\mu_0 \leq M$ for some finite M . Then the distribution at the iteration t of the MCMC algorithm satisfies $d\pi/d\mu_t \leq M$.

Proof. We have

$$\begin{aligned} \frac{d\pi}{d\mu_t}(x_t) &= E \left\{ \frac{d(\pi \times K^t)}{d(\mu_0 \times K^t)}(X_0, X_t) \mid X_t = x_t \right\} \\ &\leq E \left\{ M \frac{dK^t(x_0, \cdot)}{dK^t(x_0, \cdot)}(X_t) \mid X_t = x_t \right\} \leq M. \end{aligned}$$

□

To prove Corollaries 3 and 4, we need to verify Assumptions 2 and 3 on the system of particles $X_t^{1:N}$ and weights $W_t^{1:N}$ so that Theorem 1 can be applied. Using Theorem 2, Assumption 2 is fulfilled if

$$E_\pi \left[f' \left\{ \frac{d\pi}{d\mu_t}(X) \right\}^4 \right] < \infty. \quad (15)$$

By the strong law of large number and the independence of X_t^i and X_t^j for $1 \leq i < j \leq N$ and $N+1 \leq i < j \leq 2N$, Assumption 3 is fulfilled if

$$E_{\pi_t} \left[\frac{d\pi}{d\mu_t}(X) \left| f' \left\{ \frac{d\pi}{d\mu_t}(X) \right\} \right| \right] < \infty; \quad (16)$$

$$E_{\pi_t} \left[\left| f \left\{ \frac{d\pi}{d\mu_t}(X) \right\} \right| \right] < \infty. \quad (17)$$

Proof of Corollary 3. Recall that $\pi(x) \leq M_1 \mu_0(x)$ for some constant M_1 . Using Lemma 5 we have $\pi(x) \leq M_1 \mu_t(x)$ as well. It is then easy to verify (15), (16) and (17) by noting that all the three functions $f'(t)$, $tf'(t)$, and $f(t)$ are bounded on $[0, M_1]$. □

Proof of Corollary 4. Recall that $\pi(x) \leq M_1 \mu_0(x)$ for some constant M_1 . Using Lemma 5 we have $\pi(x) \leq M_1 \mu_t(x)$ as well. It is then easy to verify (16) and (17) by noting that $f(t) = t \log t$ and $tf'(t) = t(\log t + 1)$ are both bounded on the interval $[0, M_1]$. To verify (15), we rewrite it for our specific KL divergence:

$$E_\pi \left[\left\{ 1 + \log \frac{\pi(X)}{\mu_t(X)} \right\}^4 \right] < \infty. \quad (18)$$

Using the regularity of kernel K , the hypothesis $\|\mu_0\|_\infty \leq M_2$, and the fact that $\pi(x) \leq M_1 \mu_t(x)$ we have

$$-\log M_1 + \log \pi(x) \leq \log \mu_t(x) \leq t \log \|K\|_\infty + M_2$$

which means

$$|\log \mu_t(x)| \leq |\log M_1| + |\log \pi(x)| + t \log \|K\|_\infty + M_2.$$

Combining this inequality with the assumption $E_\pi \{(1 + \log \pi(X))^4\} < \infty$, we obtain (18) and conclude the proof. □

I Couplings

I.1 Reflection maximal coupling

When $p(x) \sim \mathcal{N}(\mu_1, \Sigma)$ and $q(x) \sim \mathcal{N}(\mu_2, \Sigma)$ are two multivariate Gaussian densities with the same covariance matrix, it is possible to form a maximal coupling of $X \sim p$, $Y \sim q$, that is, a coupling such that $\text{pr}(X = Y)$ is maximized as per Algorithm 2. This coupling furthermore incorporates a reflection, which is known to minimize the expected meeting time of Ornstein–Uhlenbeck trajectories (Uhlenbeck and Ornstein, 1930), as those in Section 5.1.

Algorithm 2: Reflection-maximal coupling for $\mathcal{N}(\mu_1, LL^\top)$ and $\mathcal{N}(\mu_2, LL^\top)$

Input: Means μ_1, μ_2 and matrix L .
Output: A coupled pair (x, y) .

```
1  $z \leftarrow L^{-1}(\mu_1 - \mu_2)$ 
2  $e \leftarrow z/\|z\|$ 
3 Sample  $V \sim \mathcal{N}(0, I)$  and  $U \sim \mathcal{U}([0, 1])$ 
   // Independently
4 if  $\mathcal{N}(V; 0, I) U < \mathcal{N}(V + z; 0, I)$  then
5   |  $W \leftarrow V + z$ 
6 else
7   |  $W \leftarrow V - 2 \langle e, V \rangle e$ 
8  $x \leftarrow \mu_1 + LW$ 
9  $y \leftarrow \mu_2 + LW$ 
```

Algorithm 3: Coupling for the random walk kernel with pre-conditioning covariance $LL^\top = \Sigma$ and target $\pi \propto \gamma$.

Input: Positions x, y , step-size δ .
Output: A coupled pair (x, y) .

```
1  $\mu_x \leftarrow x$ 
2  $\mu_y \leftarrow y$ 
3 Sample  $x', y'$  using Algorithm 2
4 Sample a uniform  $U \sim \mathcal{U}([0, 1])$ 
5 if  $U < \alpha(x', x)$  then
6   |  $x \leftarrow x'$ 
7 if  $U < \alpha(y', y)$  then
8   |  $y \leftarrow y'$ 
```

I.2 Reflection maximal coupling for random walk Metropolis–Hastings

Given the current state, the proposal distribution for the random-walk Metropolis–Hastings algorithm is Gaussian: $q(y | x) = \mathcal{N}(y; x, \delta\Sigma)$, and the proposed state is accepted with probability $\alpha(y, x) = 1 \wedge \{\gamma(y)/\gamma(x)\}$. Different coupling systems have been proposed for this proposal (Wang et al., 2021; Papp and Sherlock, 2024). Here we take a slightly suboptimal but practical approach which consists in using the reflection maximal coupling of the proposals and then using a common uniform variate to accept or reject the proposals. This is summarized in Algorithm 3.

The resulting coupling is successful if the proposals are coupled and both are accepted.

I.3 Reflection maximal coupling of Metropolis-adjusted Langevin algorithm

Given the current state, the proposal distribution for MALA is Gaussian: $q(y | x) = \mathcal{N}(y; x + \delta/2 \Sigma \nabla \log \gamma(x), \delta\Sigma)$, and the proposed state is accepted with probability $\alpha(y, x) = 1 \wedge \{\gamma(y)q(x | y)\}/\{\gamma(x)q(y | x)\}$. Here we again take the suboptimal approach of using the reflection maximal coupling of the proposals and a common uniform variate to accept proposals. This is summarized in Algorithm 4.

Algorithm 4: Coupling for the MALA kernel with pre-conditioning covariance $LL^\top = \Sigma$ and target $\pi \propto \gamma$.

Input: Positions x, y , step-size δ .

Output: A coupled pair (x, y) .

- 1 $\mu_x \leftarrow x + \delta/2 \Sigma \nabla \log \gamma(x)$
- 2 $\mu_y \leftarrow y + \delta/2 \Sigma \nabla \log \gamma(y)$
- 3 Sample x', y' using Algorithm 2
- 4 Sample a uniform $U \sim \mathcal{U}([0, 1])$
- 5 **if** $U < \alpha(x', x)$ **then**
- 6 $x \leftarrow x'$
- 7 **if** $U < \alpha(y', y)$ **then**
- 8 $y \leftarrow y'$

The resulting coupling is again successful if the proposals are coupled and both are accepted.

I.4 Pólya-Gamma sampler

The Pólya-Gamma sampler was introduced in Polson et al. (2013) as a data augmentation Gibbs scheme for the logistic regression problem as described in Section 5.2. In its uncoupled version, given the current state $\beta \in \mathbb{R}^n$ of the parameter chain, it alternates between

1. $W_i \sim \text{PG}(1, |x_i \cdot \beta|)$, $i = 1, \dots, n$
2. $\beta \sim \mathcal{N}(\mu(W), \Sigma(W))$

where $X \in \mathbb{R}^{n \times k}$ is the matrix of k entries for the n features, $\tilde{y}_i \in \{-1/2, 1/2\}$ is the scaled outcome, W is the stacked matrix of the W_i 's, $\mu(W) = \Sigma(W_i)(X^\top \tilde{y} + B^{-1}b)$, $\Sigma(W) = X^\top \text{diag}(W)X + B^{-1}$, and $\mathcal{N}(b, B)$ is the Gaussian prior for β .

Couplings for such chains are readily available owing to the Pólya-Gamma distribution having tractable likelihood ratios $\text{PG}(x; 1, c)/\text{PG}(x; 1, c')$. In Algorithm 5, we describe such a coupling, which is the one implemented in <https://github.com/pierrejacob/unbiasedmcmc/blob/master/src/logisticregressioncoupling.cpp#L79>¹ and corresponds to implementing a rejection sampler for one variable using the other one, and, if the rejection sampler fails, sampling from the Pólya-Gamma independently for the remaining variable².

Remark 8. We note that this is not the algorithm used in Biswas et al. (2019) to produce the results of their Section 3.2. However, it resulted in *better* coupling times for both their method and ours than the one described therein (Biswas et al., 2019, Algorithm 7) and is the default choice in their available code at https://github.com/niloyb/LlagCouplings/blob/master/logistic_regression/polya_gamma.R#L45³.

The full coupled sampler is then given by Algorithm 6.

¹retrieved on 08/10/2025

²Private communication with Pierre Jacob

³retrieved on 08/10/2025

Algorithm 5: Maximal coupling of P'olya–Gamma variables. Let the log of the unnormalised P'olya–Gamma density kernel be $h(z, \omega) = \log \cosh(z/2) - \frac{1}{2}z^2\omega$.

Input: Distributions $\text{PG}(1, c_1)$, $\text{PG}(1, c_2)$.

Output: Coupled samples (ω_1, ω_2) from the Pólya–Gamma distributions.

```

1 Draw  $\omega_1 \sim \text{PG}(1, c_1)$ 
2 Draw  $U_1 \sim \mathcal{U}(0, 1)$ 
3 if  $\log(U_1) \leq h(c_2, \omega_1) - h(c_1, \omega_1)$  then
4    $\omega_2 \leftarrow \omega_1$ 
5 else
6   repeat
7     Draw  $\omega'_2 \sim \text{PG}(1, c_2)$ 
8     Draw  $U_2 \sim \mathcal{U}(0, 1)$ 
9   until  $\log(U_2) > h(c_1, \omega'_2) - h(c_2, \omega'_2)$ 
10   $\omega_2 \leftarrow \omega'_2$ 

```

Algorithm 6: P'olya–Gamma Gibbs Coupling Step.

Input: Current states $\beta, \hat{\beta} \in \mathbb{R}^d$.

Output: Next states $\beta', \hat{\beta}' \in \mathbb{R}^d$.

```

1 for  $i = 1, \dots, n$  do
2   | Sample  $(W_i, \hat{W}_i)$  from Algorithm 5 for  $\text{PG}(1, |x_i^\top \beta|)$  and  $\text{PG}(1, |x_i^\top \hat{\beta}|)$ .
3 Sample  $(\beta', \hat{\beta}')$  from a maximal coupling of  $\mathcal{N}(\mu(W), \Sigma(W))$  and  $\mathcal{N}(\mu(\hat{W}), \Sigma(\hat{W}))$ .

```

We refer to Jacob et al. (2020b); Biswas et al. (2019, Section S4 and Algorithm 7, respectively) for details.

I.5 Other samplers and couplings

A large collection of couplings have been proposed for different MCMC kernels over the past decade or so. While we do not expect this list to be exhaustive, we have collected here several of them which seem to cover most of the techniques employed.

1. Hamiltonian Monte Carlo (HMC Neal, 2011) MCMC is perhaps one of the most used MCMC algorithm. It is worth noting that no exact coupling of the method has been proposed to date. In Heng and Jacob (2019), the authors instead implement a two-scale coupling of a mixture of HMC and of a random-walk. The HMC component is then made to contract in space using techniques akin to the reflection of Section I.1 while the random walk is used to eventually try and make the chains stick once they are close enough. This is a case of a two-scale coupling, where an algorithm is made to behave differently when the states are far apart versus when they are close.
2. Piecewise deterministic Markov processes (Bierkens et al., 2019, 2020; Bouchard-Côté et al., 2018) are classes of continuous-time Markov chains on a joint position-velocity state-space with tractable dynamics between velocity jumps, which may be coupled too (Corenflos et al., 2025). The underlying technique relies mostly on *clock synchronization*: managing the time and type of the jump events to control the dynamics of the process. These couplings are however less efficient than for discrete-time dynamics owing to their largely more rigid structure.
3. Optimal transport (see, e.g., Villani, 2009; Peyré and Cuturi, 2019) contraction is commonly used in order to enforce geometric (in the squared Euclidean distance sense) proximity, either for a subpart of the sampler (Nguyen et al., 2022, in the context of a Gibbs scheme for instance), or as part of a two-scale method (Biswas et al., 2022; Ceriani and Zanella, 2024), where the two chains are brought closer together, and then the optimal transport coupling is swapped for one that may make the chains meet exactly.
4. Gibbs(-like) couplings in general can be designed or studied component-wise or in a collapsed manner (Ceriani and Zanella, 2024), sometimes reaching different conclusions. A class of such samplers which has attracted a lot of research over the past few years is conditional sequential Monte Carlo methods (Jacob et al.,

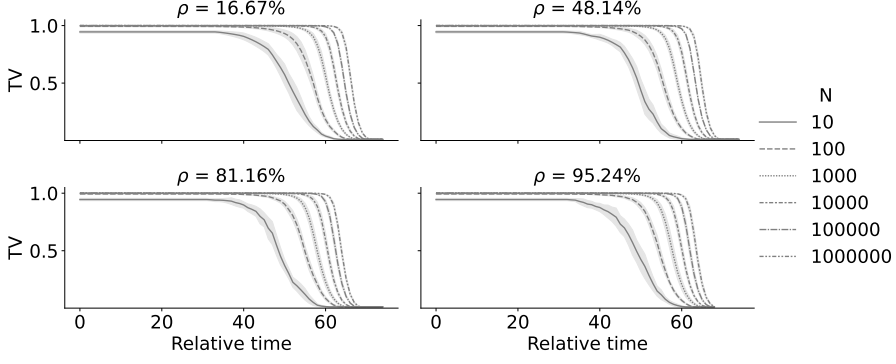


Figure 5: Total variation monitoring of the chains, the organization is the same as in Figure 2 except that no theoretical line is shown.

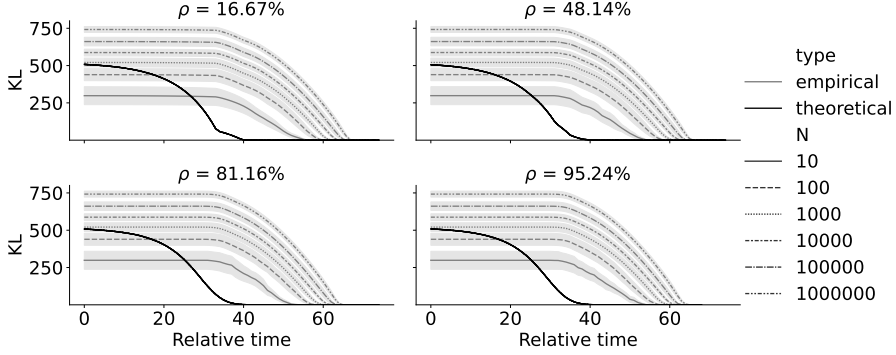


Figure 6: Kullback–Leibler monitoring of the chains, the organization is the same as in Figure 2.

2020a; Lee et al., 2020; Karjalainen et al., 2023), which, in some sense, extend Metropolis-within-Gibbs methods to systems with tractable Markovian dependencies.

5. Pseudo-marginal MCMC (Andrieu and Roberts, 2009) algorithms have also been the subject of research and their couplings have been studied in (Middleton et al., 2019, 2020). The general idea is often to design two different couplings, one for the latent state used in acceptance, and the other for the proposal distribution used for the parameter of interest.

Other uses of couplings we did not mention in this article include multilevel Monte Carlo (see, e.g., Giles, 2015; Rhee and Glynn, 2015; Vihola, 2018) or coupling from past (see, e.g., Propp and Wilson, 1996; Huber, 2016).

J Other empirical outputs

J.1 Gaussian additional statistics

We now report other computed f -divergences based on our weight-harmonization procedure. In Figure 5, the total variation is computed by itself owing to no closed form solutions being available in general, in Figure 6 we report the Kullback–Leibler divergence profile, while in Figure 7, we report the squared Hellinger distance profile.

A point of note is that the Kullback–Leibler is strongly biased compared to its χ^2 , counterparts. This is because, contrary the other f -divergences, the derivative of $f(t) = t \log t$ is unbounded at 0, so that, during early iterations, some weights being very small, regularity criteria necessary for Theorem 1 scarcely hold.

Apart from this, no qualitative difference can be seen compared to the discussion in Section 5.1: convergence can be monitored using one or another of the divergences.

J.2 Pólya-Gamma sampler additional statistics

In Figure 8, we report additional statistics for several f -divergences: the total variation distance, Kullback–Leibler divergence, the reversed Kullback–Leibler divergence, and the χ^2 and squared Hellinger distances. As expected,

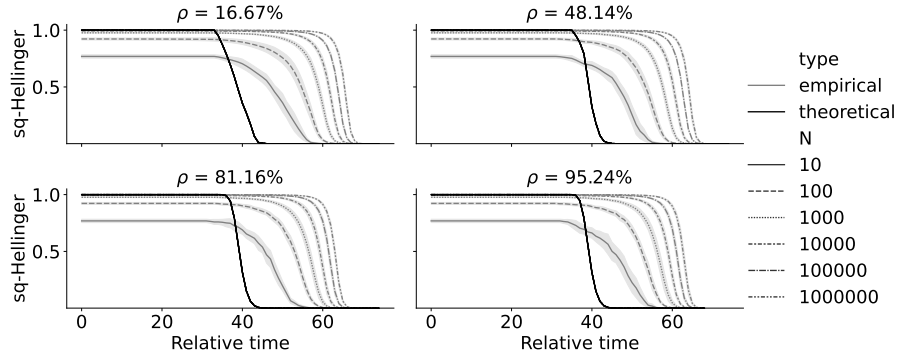


Figure 7: Squared Hellinger distance monitoring of the chains, the organization is the same as in Figure 2.

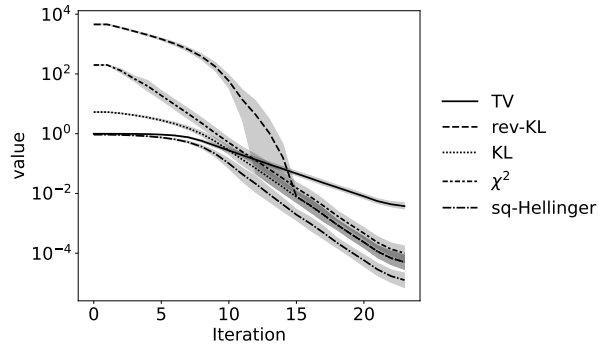


Figure 8: Different f -divergences for the German credit example of Section 5.2, given as mean ± 2 standard deviations computed over 20 independent experiments.

all these tell the same story: the chain converges in roughly 20 steps and the statistics are independent of the initialization.